



# Landslide susceptibility mapping of Cekmece area (Istanbul, Turkey) by conditional probability

T. Y. Duman<sup>1</sup>, T. Can<sup>2</sup>, C. Gokceoglu<sup>3</sup>, and H. A. Nefeslioglu<sup>1</sup>

<sup>1</sup>General Directorate of Mineral Research and Exploration, Department of Geological Research, 06520 Ankara, Turkey

<sup>2</sup>Cukurova University, Department of Geological Engineering, 01330 Balcali, Adana, Turkey

<sup>3</sup>Hacettepe University, Department of Geological Engineering, Applied Geology Division, 06532 Beytepe, Ankara, Turkey

Received: 29 November 2004 – Accepted: 17 January 2005 – Published: 19 January 2005

Correspondence to: C. Gokceoglu (cgokce@hacettepe.edu.tr)

© 2005 Author(s). This work is licensed under a Creative Commons License.

Landslide  
susceptibility  
mapping of Cekmece

T. Y. Duman et al.

Title Page

Abstract

Introduction

Conclusions

References

Tables

Figures

◀

▶

◀

▶

Back

Close

Full Screen / Esc

Print Version

Interactive Discussion

EGU

As a result of industrialization, throughout the world, the cities have been growing rapidly for the last century. One typical example of these growing cities is Istanbul. Today, the population of Istanbul is over 10 millions. Depending on this rapid urbanization, new suitable areas for settlements and engineering structures are necessary. For this reason, the Cekmece area, west of the Istanbul metropolitan area, is selected as the study area, because the landslides are frequent in this area. The purpose of the present study is to produce landslide susceptibility map of the selected area by conditional probability approach. For this purpose, a landslide database was constructed by both air – photography and field studies. 19.2% of the selected study area is covered by landslides. Mainly, the landslides described in the area are generally located in the lithologies including the permeable sandstone layers and impermeable layers such as claystone, siltstone and mudstone layers. When considering this finding, it is possible to say that one of the main conditioning factors of the landslides in the study area is lithology. In addition to lithology, many landslide conditioning factors are considered during the landslide susceptibility analyses. As a result of the analyses, the class of 5–10° of slope, the class of 180–225 of aspect, the class of 25–50 of altitude, Danismet formation of the lithological units, the slope units of geomorphology, the class of 800–1000 m of distance from faults (DFF), the class of 75–100 m of distance from drainage (DFD) pattern, the class of 0–10 m of distance from roads (DFR) and the class of low or impermeable unit of relative permeability map have the higher probability values than the other classes. When compared with the produced landslide susceptibility map, most of the landslides identified in the study area are found to be located in the most (54%) and moderate (40%) susceptible zones. This assessment is also supported by the performance analysis applied at end of the study. As a consequence, the landslide susceptibility map produced herein has a valuable tool for the planning purposes.

### Landslide susceptibility mapping of Cekmece

T. Y. Duman et al.

[Title Page](#)

[Abstract](#)

[Introduction](#)

[Conclusions](#)

[References](#)

[Tables](#)

[Figures](#)

◀

▶

◀

▶

[Back](#)

[Close](#)

[Full Screen / Esc](#)

[Print Version](#)

[Interactive Discussion](#)

EGU

## 1. Introduction

---

### Landslide susceptibility mapping of Cekmece

T. Y. Duman et al.

---

[Title Page](#)

[Abstract](#)

[Introduction](#)

[Conclusions](#)

[References](#)

[Tables](#)

[Figures](#)

[◀](#)

[▶](#)

[◀](#)

[▶](#)

[Back](#)

[Close](#)

[Full Screen / Esc](#)

[Print Version](#)

[Interactive Discussion](#)

Doyuran, 2004a; Ayalew and Yamagishi, 2004), probabilistic approach (Gritzner et al., 2001; Rowbotham and Dudycha, 1998; Clerici et al., 2002), neural networks (Lee et al., 2001, 2003 and 2004; Gomez and Kavzoglu, 2004) and fuzzy approach (Juang et al., 1992; Binaghi et al., 1998; Ercanoglu and Gokceoglu, 2002 and 2004). It is evident that each landslide susceptibility assessment method considered by landslide community has some advantages and drawbacks. For this reason, among the landslide researchers, there is no agreement either on the methods or on the scope of producing hazard maps (Brabb, 1984). Surprisingly, Brabb's idea (Brabb, 1984) is still valid for the techniques employed in landslide susceptibility mapping studies, because regional landslide susceptibility assessments pose complex problems due to a lack of knowledge and variability.

A hundred years ago, the world population totalled 1.1 billion, and about 5% of people lived in cities. Today, the population has risen to 5.3 billion and approximately 45% of it is concentrated in urban areas. The most explosive growth has been in the developing world, where urban populations have tripled in the last 30 years. Between the years of 1950–1995, the number of cities with population of more than one million increased sixfold in the third world (Helmore, 1996; after Guzzetti et al., 1999). One typical example among the cities having explosive growth is Istanbul. This metropolitan city, located in the northern west of Turkey, is the most crowded city of Turkey with a population of above 10 million and Istanbul is also the financial and cultural centre of Turkey. At the same time, it is a city world-famous for its natural beauty and historical monuments, reflecting its role as the capital of three separate empires. It enjoys the unique amenities of shorelines on the Black Sea, the Marmara Sea and the Bosphorus Strait. The rapid growth of the city since the 1950s, due to rural migration, has affected the quality of life in various sections of the city (Dokmeci and Berkoz, 2000). Due to this rapid growth of Istanbul, new settlement areas are needed and the study area is one of the new settlement areas of Istanbul. In the study area (Fig. 1), new tall apartments, houses having two or three storeys and factories are constructed. Moreover, as a result of urbanization, new roads, highways and lifelines are built up.

## Landslide susceptibility mapping of Cekmece

T. Y. Duman et al.

[Title Page](#)

[Abstract](#)

[Introduction](#)

[Conclusions](#)

[References](#)

[Tables](#)

[Figures](#)

[◀](#)

[▶](#)

[◀](#)

[▶](#)

[Back](#)

[Close](#)

[Full Screen / Esc](#)

[Print Version](#)

[Interactive Discussion](#)

EGU

As can be seen in Fig. 2, many structures in the study area are constructed in active landslides and/or the areas susceptible to landsliding. For this reason, preparation of a realistic landslide susceptibility map for the planning and correct site selection purposes is indispensable. Generally, the landslide susceptibility maps help to planners and decision – makers for correct site selection and planning. For this reason, in this study, production of landslide susceptibility map of a part of Istanbul, Cekmece area is aimed considering conditional probability method. This study is composed of four main stages such as (a) preparation of landslide inventory by air – photography studies, (b) field checks of landslide inventory, (c) preparation of index maps of the study area and 10 production of landslide susceptibility map, and (d) assessment of performance of the produced landslide susceptibility map.

## 2. General properties of the study area

The study area locates at the northern coast of the sea of Marmara and western part of Istanbul metropolitan area (see Fig. 1). The Buyuk Cekmece lake, and the Kucuk Cekmece lake and Dikilitas creek are the western and eastern borders of the study 15 area, respectively. The study area is in the Marmara region having a high – seismicity. Recently, Turkey has experienced some large earthquakes. The 17 August 1999 Izmit earthquake on the NAF's northern branch has also increased the earthquake risk in the Sea of Marmara (Parsons et al., 2000). More than 300 earthquakes are reported to 20 have occurred between 2100 BC and AD 1900 (Soysal et al., 1981). The active northern branch of the Northern Anatolian Fault Zone (NAFZ) passes through the distance of 9 km from south of the study area. In the last 20 centuries, between Izmit and Gulf of Saros, 29 historically large (between 6.3 and 7.4  $M_s$ ) earthquakes occurred along the northern branch NAFZ (Ambraseys, 2002). One of the main landslide triggers is 25 earthquakes while the other is heavy rainfall. The seismicity of the study area becomes one of these triggers.

In the stratigraphic succession, the Kirkklareli limestone, the oldest rocks of the study

---

### Landslide susceptibility mapping of Cekmece

T. Y. Duman et al.

---

[Title Page](#)

[Abstract](#)

[Introduction](#)

[Conclusions](#)

[References](#)

[Tables](#)

[Figures](#)

◀

▶

◀

▶

[Back](#)

[Close](#)

[Full Screen / Esc](#)

[Print Version](#)

[Interactive Discussion](#)

EGU

## Landslide susceptibility mapping of Cekmece

T. Y. Duman et al.

[Title Page](#)

[Abstract](#)

[Introduction](#)

[Conclusions](#)

[References](#)

[Tables](#)

[Figures](#)

[◀](#)

[▶](#)

[◀](#)

[▶](#)

[Back](#)

[Close](#)

[Full Screen / Esc](#)

[Print Version](#)

[Interactive Discussion](#)

EGU

area of the Middle-Late Eocene, observed in the eastern parts of the study area. The Ihsaniye formation, interfingered with the Kirkclareli limestone, consists of sedimentary units such as shale-marls of the Late Eocene-Early Oligocene observed in the northern parts of the study area (Fig. 3). The Danismert formation of Late Oligocene includes 5 alternation of sandstone, shale and marl with thin-moderate beddings (Fig. 4) (Duman et al., 2004). This formation is observed at the western parts of the study area. Sandstone and shale alternation bearing gypsum and coal layers comprising the Suloglu formation is interfingered with the Danismert formation. Tuffs, sandstones and gravelstones form the Cantakoy formation, appear in the southwestern and southern parts of 10 the area. The age of the Cantakoy formation is Early Miocene. The Ergene formation unconformably lie over the Cantakoy formation. The age of the Ergene formation is Middle Miocene and it consists of sandstones and gravelly sandstones. This formation is observed at northern and southern parts of the area. The Bakirkoy formation, represented by limestones and claystones, crops out middle parts of the area (Fig. 3). The 15 age of the Bakirkoy formation is Late Miocene (Safak et al., 1999). The terraces unconformably covers the oldest rocks and it is observed at the coast of Buyuk Cekmece lake. The youngest unit in the study area is actual alluviums.

In the area, some inactive normal faults are typical. The direction of these faults are generally northeast - southwest, but that of the most important normal fault, Yesilbayir 20 fault, is roughly northwest – southeast (Duman et al., 2004). These faults can be observed in the Miocene lithologies in the area. The dip values of the beddings of the sedimentary units in the area are rather low, 5–15°. For this reason, the strikes and the dip directions exhibit a high variation in short distances. However, in the study area, there is no considerable folding.

25 The altitude values vary between 0–200 m while the dominant altitude ranges are 75–100 and 100–125 m (Figs. 5a and 5b). The study area has a dendritic drainage pattern, because of presence of soft lithologies and low slope angles. The general physiographic trend of the study area is NW–SE as can be seen in Figs. 6a and 6b. Although the range of slope angle values is 0 to 90°, the majority of them are between

0–20° (Figs. 7a and 7b). These slope values indicate that the majority of the area has gentle slopes.

The geomorphology map of the study area was produced by Duman et al. (2004) (Fig. 8). In the study area, denudation and pediment surfaces, slope zones, transition zones, alluvial floors and coastal zones form the main geomorphological units. Considering the purpose of the present study, the most important geomorphological units are the slope zones contributing the landslides occurrence. Especially, lower borders of the Late Miocene eroding surfaces are the failure surfaces of the landslides in the region (Duman et al., 2004). In addition, a dense landslide occurrence can be observed at the slope zones near the coast lines of the lakes and the Sea of Marmara in the area.

According to the relative permeability map of the lithologies prepared by Duman et al. (2004), considering the classification of proposed by Todd (1980), permeable, semi – permeable and impermeable units exist in the area (Fig. 9). Mainly, the eastern and southern parts of the area have permeable units while impermeable and semi – permeable units are dominant at the western and northern parts of the area. In the area, there are many springs. These springs discharge along the borders of permeable and semi or impermeable units. This indicates that the permeable units have a considerable groundwater. The main streams in the study area are the Dikilitas creek, Cekmece creek, Uzuncayir creek and Harami creek. The general stream direction of the Cekmece creek and Uzuncayir creek in the study area is from northeast to southwest and they discharge to the Cekmece lake while that of Dikilitas creek is northwest to southeast and it discharges to the Sea of Marmara. Besides, there are many lower order streams flowing only after rainy periods and their flowing directions are generally southwest.

In the region, the Marmara and Western Black Sea climate prevails. Generally, in the summer season, the weather is hot and slightly rainy while the weather of winter seasons is warm and rainy. The topography of the region and presence of lakes and dams affect the weather conditions (<http://istanbul.meteor.gov.tr>). The region receives 85% of the total annual precipitation in rainy season, September–May (<http://istanbul>.

Landslide susceptibility mapping of Cekmece

T. Y. Duman et al.

[Title Page](#)

[Abstract](#)

[Introduction](#)

[Conclusions](#)

[References](#)

[Tables](#)

[Figures](#)

◀

▶

◀

▶

[Back](#)

[Close](#)

[Full Screen / Esc](#)

[Print Version](#)

[Interactive Discussion](#)

meteor.gov.tr). In this study, the data of Florya Meteorology Station, the nearest station to the study area, was employed. According to the meteorological data of the period of 1937–1990, the average monthly rainfall varies between 20.5 mm and 102.0 mm (Fig. 10). The annual precipitation varies between 500 mm and 1000 mm in the region while average annual precipitation of long period of the Florya Meteorology Station is 642.4 mm (DMI, 1990). The average monthly temperature varies from 5.3°C to 23.2°C. The coldest month is January with average temperature of 5.3°C and the hottest month is July with average temperature of 23.2°C. In winter seasons particularly, the region sometimes receive heavy precipitation causing some floods and triggering landslides.

10 The maximum daily precipitation recorded in the period of 1937–1990 varies between 43.8 mm and 112.5 mm (DMI, 1990). When 112.5 mm is considered, the maximum rainfall intensity is calculated as 4.7 mm/h. As a consequence, the region has the landslide triggers such as earthquake and heavy precipitation. However, in this study, the conditioning factors are only taken into consideration when producing landslide

15 susceptibility map.

### 3. Landslide characteristics

In the hope that the geomorphologic conditions of a specific dynamic type of mass movement (e.g. shallow translational landslides, debris flows, rock falls) can be sufficiently described by corresponding combinations of basic thematic maps (e.g. topographic slope, land cover, lithological units, distribution of past landslides) spatial databases need to be constructed for analysing and modelling by geographical information systems (GIS) (Fabbri et al., 2003). In general, mapping past and recent slope movements, together with the identification and mapping of the conditioning or preparatory factors of slope instability, are the keys in predicting future landslides (Carrara et al., 1998). A reliable landslide inventory defining the type and activity of all landslides, as well as their spatial distribution, is essential before any analysis of the occurrence of landslides and their relationship to environmental conditions undertaken (Soeters

## Landslide susceptibility mapping of Cekmece

T. Y. Duman et al.

[Title Page](#)

[Abstract](#)

[Introduction](#)

[Conclusions](#)

[References](#)

[Tables](#)

[Figures](#)

◀

▶

◀

▶

[Back](#)

[Close](#)

[Full Screen / Esc](#)

[Print Version](#)

[Interactive Discussion](#)

EGU

and van Westen, 1996). Therefore, it is possible to say that a reliable landslide inventory is a crucial part of a landslide susceptibility map among the parameters employed, because it is the fundamental component of the assessments.

In Turkey, there are no a landslide inventory at the national scale. For this reason, in this study, a landslide inventory was prepared by using the vertical black-and-white aerial photographs of medium scale (1:35 000), dated 1955–1956, were used to identify the landslides. When describing the type and activity of the landslides in the study area, the similar criteria defined in the Turkish Landslide Inventory Mapping Project initiated by the Natural Hazards and Environmental Geology division of the General Directorate of Mineral Research and Exploration (MTA) were considered. In this project (Duman et al., 2001), mass movements were classified according to the main types of classification proposed by Varnes (1978), i.e. flows, falls and slides. The landslides are also classified according to their relative depths, as shallow – (depth <5 m) and deep-seated (depth >5 m). For simplicity, their activities are classified into two groups as active and inactive. Active landslides are defined as those currently moving, whereas inactive ones are as relict according to WP/WLI (1993). Shallow landslides are classified as active because of their ongoing observed movements (Duman et al., 2005). The landslide locations described in the air-photography studies were controlled by field studies. One of the most important stages of landslide susceptibility mapping is to describe the factors governing the landslides identified in the area. To complete this stage, an extensive field study is needed to describe the mechanisms, activity and conditioning factors of landslides. For this purpose, in this study, following the air-photography studies, a field study was conducted. During the field studies, some observations were carried out on the areal extent of landslides and their mechanisms. The characters of landslides identified in the area are mainly deep seated and active.

The landslides are the most frequent in the selected study area when compared with the Trakya region. The described landslides are generally located in the lithologies including the permeable sandstone layers and impermeable layers such as claystone, siltstone and mudstone layers. This is typical for the landslides identified in the study

## Landslide susceptibility mapping of Cekmece

T. Y. Duman et al.

[Title Page](#)

[Abstract](#)

[Introduction](#)

[Conclusions](#)

[References](#)

[Tables](#)

[Figures](#)

[◀](#)

[▶](#)

[◀](#)

[▶](#)

[Back](#)

[Close](#)

[Full Screen / Esc](#)

[Print Version](#)

[Interactive Discussion](#)

EGU

area. When considering this finding, it is possible to say that one of the main conditioning factors of the landslides in the study area is lithology. This can be seen clearly in Fig. 11. As can be seen in Fig. 11, the majority of the landslides (approximately 60%) occurred in two formations such as Danismert formation – Acmalar member (Toda) and Ergene (Tme) formations. An another factor governing the landslides is the sandstone bedding planes and their orientations. If there is a daylight between the orientation of slope and bedding plane, some large landslides occur (Fig. 12). In these areas, the beginning of the landslides are controlled by the bedding planes as planar failure, and then in the displaced and accumulated material, some rotational landslides are observed (Fig. 13). Rarely, in this material, some earthflows may occur depending on the heavy rainfalls. The average failure surface depth of the landslides described in the study area is about 15 m (Arpat, 1999). Based on cross-sections, however, the estimated maximum failure are about 20–25 m. The pixel number of the landslide areas is 53674, this indicates that 19.2% of the study area is covered by the landslides.

The most important topographical factor conditioning landslides is the slope angle. In the regional landslide susceptibility or hazard assessments, several researchers (Roth, 1983; Barisone and Bottino, 1990; Koukis and Ziourkas, 1991; Anbalagan, 1992; Pachauri and Pant, 1992; Maharaj, 1993; Jager and Wieczorek, 1994; Anbalagan and Singh, 1996; Atkinson and Massari, 1998; Baum et al., 1998; Guzzetti et al., 1999; Zezere et al., 1999; Guzzetti et al., 2000; Jakob, 2000; Nagarajan et al., 2000) took into consideration statistical techniques for the assessment of slope angle in terms of landslide activity. In the study area, the frequency of the identified landslides reached peak value at the slope angle range of 5–15° (Fig. 14) and the slope angle is considered as a conditioning factor during the analyses.

Although the relation between slope aspect and mass movement has long been investigated, no general agreement exists on slope aspect (Carrara et al., 1991). Several authors (i.e. Carrara et al., 1991; Maharaj, 1993; Gokceoglu and Aksoy, 1996; Jakob, 2000; Nagarajan et al., 2000) considered the slope aspect as a factor conditioning the landslides. Mainly, the slope aspect is related to the general physiographic trend of the

## Landslide susceptibility mapping of Çekmece

T. Y. Duman et al.

[Title Page](#)

[Abstract](#)

[Introduction](#)

[Conclusions](#)

[References](#)

[Tables](#)

[Figures](#)

◀

▶

◀

▶

[Back](#)

[Close](#)

[Full Screen / Esc](#)

[Print Version](#)

[Interactive Discussion](#)

EGU

area and/or the main precipitation direction. The relationship between direction of the landslides and general physiographic trend of the area should be roughly perpendicular. The general physiographic trend of the area is NW–SE and an important part of the landslides observed in the area studied has failure directions to NE and NW (Fig. 15).

5 Some authors (i.e. Pachauri and Pant, 1992; Ercanoglu and Gokceoglu, 2002) reported that the altitude is a good indicator for the landslide susceptibility assessments. However, in the area studied, there is no a considerable difference between the lowest and the highest altitude values, 200 m. For this reason, there is no an agreement between landslide frequency and altitude (Fig. 16). Even though this finding, the altitude  
10 is taken into consideration in the analyses.

It can be thought as the structural elements such as faults, folds, joints or some parts of them, make the materials where landslides occur more susceptible to sliding because of material weakening, stress accumulation or tectonic activity in different distances. However, there is not a consensus among the researchers about the distances from the structural elements to be considered. As a result, the researchers  
15 have used different distances with respect to the closeness to the structural elements in the literature (Anbalagan, 1992; Pachauri and Pant, 1992; Maharaj, 1993; Gokceoglu and Aksoy, 1996; Luzi and Pergalani, 1999; Donati and Turrini, 2002; Ercanoglu and Gokceoglu, 2004). In this study, inactive faults in the study area are considered as the  
20 structural elements and the distances of 0–200, 200–400, 400–600, 600–800, 800–1000, and >1000 m to the faults are buffered (Fig. 17) and the landslide distribution in these buffer zones is shown in Fig. 18. It is evident that the majority of the landslides locates in the zone of >1000 m. However, the class of >1000 m is accepted as the  
25 zone unaffected from the faults. For this reason, during the analyses, the probability of this class is accepted as zero.

One of the important factors conditioning the landslides is the proximity to the drainage pattern, because streams may adversely affect the stability by either eroding the toe or saturating the slope material or both (Gokceoglu and Aksoy, 1996). For this reason, this parameter is also evaluated by creating buffer zones of 0–25, 25–50,

## Landslide susceptibility mapping of Cekmece

T. Y. Duman et al.

[Title Page](#)

[Abstract](#)

[Introduction](#)

[Conclusions](#)

[References](#)

[Tables](#)

[Figures](#)

◀

▶

◀

▶

[Back](#)

[Close](#)

[Full Screen / Esc](#)

[Print Version](#)

[Interactive Discussion](#)

EGU

50–75, 75–100, 100–125, and >125 m (Fig. 19), and the results is given in Fig. 20. However, there is no an agreement between the landslide density and the proximity to drainage pattern. 85.3% of the landslides accumulate in the class of >125 m. However, this class is not considered during the analyses.

5 In addition to the lithological features, the relative permeability map of the units is taken into consideration as the conditioning factors of the landslides. One of the main conditioning factors is permeability characteristic of the units (Fig. 21). 88.6% of the landslides is in the class of >50 m of the distance from roads (Fig. 22 and Fig. 23). This is typical for all the parameters having the line character such as roads, faults and  
10 drainage pattern. Due to the fact that this line character, the class of >50 m is not taken into consideration during the analyses. The geomorphological units and land – units are considered in the landslide susceptibility analyses (Fig. 24). As an expected result, most of the landslides locate in the slopes while minority of them is observed in the landslide morphology (PH) and Upper Miocene infilling surfaces (UMDY).

#### 15 4. Methodology

In the present study, the digital elevation model (DEM) was produced by digitizing 10 m altitude contours of the 1/25 000 scaled topographical maps. The slope, aspect and altitude maps obtained from the DEM are raster maps with a pixel size of 25×25 m. However, the other maps such as lithology, geomorphology, distance from faults, distance from drainage, distance from roads, relative permeability and landslide inventory  
20 are vector maps, and these maps were converted to raster maps with a pixel size of 25×25 m for the implementation in the susceptibility analyses.

Landslide susceptibility evaluation involves a high level of uncertainty due to data limitations and model shortcomings (Zezere, 2002). For this reason, the landslide researchers have considered different techniques for preparation landslide susceptibility maps as mentioned in the introduction chapter of this paper. One of these techniques  
25 is statistical analyses. Among the statistical techniques, a special place is held by Con-

## Landslide susceptibility mapping of Cekmece

T. Y. Duman et al.

[Title Page](#)

[Abstract](#)

[Introduction](#)

[Conclusions](#)

[References](#)

[Tables](#)

[Figures](#)

[◀](#)

[▶](#)

[◀](#)

[▶](#)

[Back](#)

[Close](#)

[Full Screen / Esc](#)

[Print Version](#)

[Interactive Discussion](#)

EGU

---

## Landslide susceptibility mapping of Çekmece

---

T. Y. Duman et al.

---

[Title Page](#)

[Abstract](#)

[Introduction](#)

[Conclusions](#)

[References](#)

[Tables](#)

[Figures](#)

[◀](#)

[▶](#)

[◀](#)

[▶](#)

[Back](#)

[Close](#)

[Full Screen / Esc](#)

[Print Version](#)

[Interactive Discussion](#)

EGU

ditional Analysis, a conceptually simple technique which is highly compatible with GIS operating features and produces results that can easily be assessed by non-specialists (Clerici et al., 2002). This method is profitably applied in relation to a particular land surface subdivision in the so-called Unique Condition Units (Carrara et al., 1995), Unique Condition Subareas (Chung et al., 1995) or pixels. Mainly the probability that event A will occur if event B occurs is called the conditional probability (Negnevitsky, 2002). More specifically, the conditional probability approach considers a number of factors governing the landslides, which are thought to be strictly connected with landslide occurrence. The data layers, in which each factor is subdivided into a convenient number of classes, are crossed in order to obtain all the possible combinations of the various classes of the different factors (Clerici et al., 2002). Each specific combination represents a pixel. Subsequently, the landslide spatial frequency, usually represented by the landslide density, is determined within each pixel. Assuming the already mentioned principle that slope-failure in the future will be more likely to occur under those conditions which led to past instability and working on the statistical concept whereby the frequency of an event, the density of an event, equals the probability that the same event will occur, the resulting landslide density equals the landslide susceptibility (Clerici et al., 2002). Conditional probability is denoted mathematically as  $p(A|B)$  (Eq. 1) (Negnevitsky, 2002).

20 
$$P(A|B) = (\text{the number of times } A \text{ and } B \text{ can occur}) / (\text{the number of times } B \text{ can occur}). \quad (1)$$

The number of times A and B can occur, or the probability that both A and B will occur, is also called “joint probability” of A and B. It represents mathematically as  $P(A \cap B)$ . The number of ways B can occur is the probability of B,  $P(B)$ ;

$$P(A|B) = P(A \cap B) / P(B). \quad (2)$$

25 Similarly, the conditional probability of event B occurring given that event A has occurred equals;

$$P(B|A) = P(B \cap A) / P(A). \quad (3)$$

Hence,

$$P(B \cap A) = P(B|A) \times P(A). \quad (4)$$

The joint probability is commutative, thus;

$$P(A \cap B) = P(B \cap A), \quad (5)$$

5 therefore,

$$P(A|B) = [P(B|A) \times P(A)]/P(B). \quad (6)$$

The last equation (Eq. 6) is known as the Bayesian rule. This principle can be extended to event A being dependent on a number of mutually exclusive events  $B_1, B_2, \dots, B_n$ . The following set of equations can then be derived from Eq. (2):

10  $P(A \cap B_1) = P(A|B_1) \times P(B_1)$

$$P(A \cap B_2) = P(A|B_2) \times P(B_2)$$

:

:

$$P(A \cap B_n) = P(A|B_n) \times P(B_n)$$

15 or, when combined;

$$P(A) = \sum_{i=1}^n P(A \cap B_i) = \sum_{i=1}^n P(A|B_i) \times P(B_i). \quad (7)$$

In the present study, Eq. (7) was employed to obtain the final susceptibility map of the area.

20 The limitations of this approach are summarized by Clerici et al. (2002). According to these researchers (Clerici et al., 2002), one such limitation is the necessity to introduce a limited number of factors subdivided into a limited number of classes into

## Landslide susceptibility mapping of Cekmece

T. Y. Duman et al.

[Title Page](#)

[Abstract](#)

[Introduction](#)

[Conclusions](#)

[References](#)

[Tables](#)

[Figures](#)

◀

▶

◀

▶

[Back](#)

[Close](#)

[Full Screen / Esc](#)

[Print Version](#)

[Interactive Discussion](#)

EGU

the analysis. Otherwise, a high number of pixels of small dimensions, and so of little statistical significance, could result from the crossing of the data layers. But probably the most limiting aspect is that an eventual change of the factors, or simply their reclassification, implies restarting the entire procedure which, however conceptually simple it

5 may be, is nevertheless complicated to execute. To overcome this difficulty, Clerici et al. (2002) have produced a shell program (or shell script) that executes the procedure automatically making it, therefore, possible to repeat it quickly and with limited user involvement.

In recent years, the conditional probability approach has been applied successfully 10 to produce landslide susceptibility maps by researchers (Clerici et al., 2002; Suzen and Doyuran, 2004a; Lee, 2004). According to the findings of Suzen and Doyuran (2004b) and Lee (2004), the logical regression analysis seems to be more consistent when 15 compared with the conditional probability. However, the application of conditional probability to the production of landslide susceptibility maps is easy; the process of input, calculation, and output can be readily understood. Also, the speed of bivariate methods could be said to be an advantage over multivariate methods (Suzen and Doyuran, 2004b). For these reasons, the conditional probability approach is preferred to prepare the landslide susceptibility map of Cekmece area.

In the first stage of the application of the conditional probability approach, the  $p(A|B)$ , 20  $p(A)$  and  $p(B)$  values are calculated (Table 1). Then, the probability values for landslide susceptibility are calculated for each pixel by summing up the  $p(A)$  values of each conditioning parameter considered in this study. Considering the probability values, the final landslide susceptibility map of the Cekmece area is produced (Fig. 25). Also, to assess the weights of the parameters visually, the weights of each parameter class 25 are calculated (Eq. 8) and given in Fig. 26.

$$w = P(A|B) - (\text{area of all landslides})/(\text{whole area}). \quad (8)$$

As can be seen in Fig. 26, some classes of the lithology, slope, aspect, altitude, geomorphology, distance from drainage and relative permeability are the most effective parameters on the landslides identified in the study area (Fig. 26).

## Landslide susceptibility mapping of Cekmece

T. Y. Duman et al.

[Title Page](#)

[Abstract](#)

[Introduction](#)

[Conclusions](#)

[References](#)

[Tables](#)

[Figures](#)

◀

▶

◀

▶

[Back](#)

[Close](#)

[Full Screen / Esc](#)

[Print Version](#)

[Interactive Discussion](#)

EGU

When making a close inspection to the produced susceptibility map, it can be observed that a considerable part of the slopes having NW–SE direction have the most susceptible zones to landsliding (Fig. 25). When compared with the produced landslide susceptibility map for the Cekmece area, all of the landslides identified in the study area are found to be located in the most (54%) and moderate (40%) susceptibility classes. As far as performance of the conditional probability approach for processing is concerned (Fig. 27), the images appear to be quite satisfactory, the zones described on the map being zones of relative susceptibility. The approach employed herein can be taken into consideration to be practical for assessing the susceptibility to landsliding.

5 The produced landslide susceptibility map will help to the decision makers during site selection and site planning processes. This map may also be accepted as a basis for the landslide risk management studies to be applied in the study area.

## 5. Results and conclusions

The following results and conclusions can be drawn from the present study.

15 The sedimentary units having different ages form the lithology of the study area are shale – marls of the Late Eocene – Early Oligocene, alternance of sandstone, shale and marl of Late Oligocene, tuffs, sandstones and gravelstones of Early Miocene, sandstones and gravelly sandstones of Middle Miocene, limestones and claystones of Late Miocene, the terraces and actual alluviums. The dip values of the beddings of these sedimentary units are rather low. For this reason, the strikes and the dip 20 directions exhibit a high variation in short distances. However, in the study area, there is no considerable folding while some inactive normal faults are typical. The direction of these faults are generally NE–SW.

25 The study area has a dendritic drainage pattern, because of presence of soft lithologies and low slope angles, and the general physiographic trend of the study area is NW–SE. The majority of the area has gentle slopes.

19.2% of the study area is covered by the landslides. The described landslides

<a href="#">Title Page</a>	
<a href="#">Abstract</a>	<a href="#">Introduction</a>
<a href="#">Conclusions</a>	<a href="#">References</a>
<a href="#">Tables</a>	<a href="#">Figures</a>
<a href="#">◀</a>	<a href="#">▶</a>
<a href="#">◀</a>	<a href="#">▶</a>
<a href="#">Back</a>	<a href="#">Close</a>
<a href="#">Full Screen / Esc</a>	
<a href="#">Print Version</a>	
<a href="#">Interactive Discussion</a>	

## Landslide susceptibility mapping of Cekmece

T. Y. Duman et al.

are typically located in the lithologies including the permeable sandstone layers and impermeable layers such as claystone, siltstone and mudstone layers. Considering this finding, it is possible to say that one of the main conditioning factors of the landslides in the study area is lithology. An another factor governing the landslides is the sandstone bedding planes and their orientations. If there is a daylight between the orientation of slope and bedding plane, some large landslides occur. In these areas, the beginning of the landslides are controlled by the bedding planes as planar failure, and then in the displaced and accumulated material, some rotational landslides are observed. Rarely, in this material, some earthflows may occur depending on the heavy rainfalls.

Altitude, slope, aspect, lithology, distance to faults, distance to drainage, distance to roads, geomorphological units and relative permeability map are considered as the conditioning factors of the landslides. The results of conditional probability analyses revealed that the classes of 5–10° of slope, the class of 180–225 of aspect, the class of 25–50 of altitude, Danismert formation – Acmalar member (Toda) of the lithological units, the slope units of geomorphology, the class of 800–1000 m of distance to faults, the class of 75–100 m of distance to drainage pattern, the class of 0–10 m of distance to roads and the class of low or impermeable unit of relative permeability map have the higher probability values than the other classes.

When compared with the so – prepared landslide susceptibility map, all of the landslides identified in the study area are found to be located in the most (54%) and moderate (40%) susceptible zones. This assessment is also supported by the performance analysis. As a consequence, the produced landslide susceptibility map can be accepted as valuable performance for the planning purposes.

The produced landslide susceptibility map will help to the decision makers during site selection and site planning processes. This map may also be accepted as a basis for the landslide risk management studies.



Ambraseys, N.: The seismic activity of the Marmara Sea region over the last 2000 years, *B Seismol. Soc. Am.*, 92, 1, 1–18, 2002.

Anbalagan, R.: Landslide hazard evaluation and zonation mapping in mountainous terrain, 5 *Engineering Geology* 32, 269–277, 1992.

Anbalagan, R. and Singh, B.: Landslide hazard and risk assessment mapping of mountainous terrains – a case study from Kumaun Himalaya, India, *Engineering Geology*, 43, 237–246, 1996.

Arpat, E.: Büyücekmece ile Kucukcekmece (İstanbul) heyelanlarının genel ozellikleri ve yarat-10 tiklari baslica sorunlar, In: *Proceedings of the 52, Turkey Geological Congress*, 17–23, 1999 (In Turkish).

Atkinson, P. M. and Massari, R.: Generalised linear modelling of susceptibility to landsliding in the Central Appenines, Italy, *Computers and Geosciences*, 24, 4, 373–385, 1998.

Ayalew, L. and Yamagishi, H.: The application of GIS-based logistic regression for landslide susceptibility mapping in the Kakuda-Yahiko Mountains, Central Japan, *Geomorphology*, 15 doi:10.1016/j.geomorph.2004.06.010, in press, 2004.

Ayenew, T. and Barbieri, G.: Inventory of landslides and susceptibility mapping in the Dessie area, northern Ethiopia, *Engineering Geology*, in press, 2004.

Baeza, C. and Corominas, J.: Assessment of shallow landslide susceptibility by means of 20 multivariate statistical techniques, *Earth Surface Processes and Landforms*, 26, 1251–1263, 2001.

Binaghi, E., Luzzi, L., Madella, P., Pergalani, F., and Rampini, A.: Slope instability zonation: a comparison between certainty factor and fuzzy Dempster – Shafer approaches, *Natural Hazards*, 17, 77–97, 1998.

25 Barisone, G. and Bottino, G.: A practical approach for hazard evaluation of rock slopes in mountainous areas, *Proceedings of the 6th Int. IAEG Cong.*, Balkema, 1509–1515, 1990.

Baum, R. L., Chleborad, A. F., and Schuster, R. L.: Landslides triggered by the winter 1996–1997 storms in the Puget Lowland, Washington, U.S. Geological Survey, Open-File Report 98-239, 1998.

30 Brabb, E. E.: Innovative approaches to landslide hazard and risk mapping, In: *Proceedings of 4th International Symposium on Landslides*, September 1984, Toronto, Canada, 1, 307–323, 1984.

## Landslide susceptibility mapping of Cekmece

T. Y. Duman et al.

[Title Page](#)

[Abstract](#)

[Introduction](#)

[Conclusions](#)

[References](#)

[Tables](#)

[Figures](#)

◀

▶

◀

▶

[Back](#)

[Close](#)

[Full Screen / Esc](#)

[Print Version](#)

[Interactive Discussion](#)

EGU

## Landslide susceptibility mapping of Cekmece

T. Y. Duman et al.

[Title Page](#)

[Abstract](#)

[Introduction](#)

[Conclusions](#)

[References](#)

[Tables](#)

[Figures](#)

◀

▶

◀

▶

[Back](#)

[Close](#)

[Full Screen / Esc](#)

[Print Version](#)

[Interactive Discussion](#)

EGU

Carrara, A., Cardinali, M., Detti, R., Guzzetti, F., Pasqui, V., and Reichenbach, P.: GIS techniques and statistical models in evaluating landslide hazard, *Earth Surface Processes and Landforms*, 16, 5, 427–445, 1991.

Carrara, A., Cardinali, M., Guzzetti, F., Reichenbach, P.: GIS based techniques for mapping 5 landslide hazard, (<http://deis158.deis.unibo.it>), 1995.

Carrara, A., Guzzetti, F., Cardinali, M., and Reichenbach, P.: Current limitations in modeling landslide hazard, In *Proceedings of IAMG'98*, edited by Buccianti, A., Nardi, G., and Potenza, R., 195–203, 1998.

Clerici, A., Perego, S., Tellini, C., and Vescovi, P.: A procedure for landslide susceptibility 10 zonation by the conditional analysis method, *Geomorphology*, 48, 349–364, 2002.

Chung, Ch., Fabbri, A. G., van Westen, C. J.: Multivariate regression analysis for landslide hazard zonation, In *Geographical Information Systems in Assessing Natural Hazards*, edited by Carrara, A. and Guzzetti, F., Kluwer Academic Publishing, Dordrecht, The Netherlands, 7–142, 1995.

15 DMI (State Meteorological Organization): Temperature and Precipitation Records of Florya Station, DMI, Ankara, 1990.

Dokmeci, V. and Berkoz, L.: Residential – location preferences according to demographic characteristics in Istanbul, *Landscape and Urban Planning*, 48, 45–55, 2000.

20 Donati, L. and Turrini, M. C.: An objective method to rank the importance of the factors pre-disposing to landslides with the GIS methodology: application to an area of the Apennines (Valnerina; Perugia, Italy), *Eng. Geol.*, 63, 277–289, 2002.

Duman, T. Y., Emre, Ö., Can, T., Ates, S., Kecer, M., Erkal, T., Durmaz, S., Dogan, A., Corekcioglu, E., Goktepe, A., Cicioglu, E., and Karakaya, F.: Turkish Landslide Inventory Mapping Project: Methodology and results on Zonguldak quadrangle (1/500000), Working in progress 25 on the Geology of Turkey and its surroundings, In: *Abstract Book of the 4th Int. Turkish Geology Symp.*, 24–28 September 2001, 392, 2001.

Duman, T. Y., Kecer, M., Ates, S., Emre, O., Gedik, I., Karakaya, F., Durmaz, S., Olgun, S., 30 Sahin, H., and Gokmenoglu, O.: Istanbul Metropolu Batisindaki (Kucukcekmece – Silivri – Catalca yoresi) Kentsel Gelisme Alanlarinin Yer Bilim Verileri, MTA, Special Publication No. 3, 249, 2004 (in Turkish).

Duman, T. Y., Can, T., Emre, Ö., Kecer, M., Dogan, A., Ates, S., and Durmaz, S.: Landslide inventory of northwestern Anatolia, *Engineering Geology*, 77, 1/2, 99–114, 2005.

Ercanoglu, M. and Gokceoglu, C.: Assessment of landslide susceptibility for a landslide-prone

## Landslide susceptibility mapping of Cekmece

T. Y. Duman et al.

[Title Page](#)

[Abstract](#)

[Introduction](#)

[Conclusions](#)

[References](#)

[Tables](#)

[Figures](#)

[◀](#)

[▶](#)

[◀](#)

[▶](#)

[Back](#)

[Close](#)

[Full Screen / Esc](#)

[Print Version](#)

[Interactive Discussion](#)

EGU

area (North of Yenice, NW Turkey) by fuzzy approach, *Environ. Geol.*, 41, 720–730, 2002.

Ercanoglu, M. and Gokceoglu, C.: Use of fuzzy relations to produce landslide susceptibility map of a landslide prone area (West Black Sea Region, Turkey), *Engineering Geology*, 75, 229–250, 2004.

5 Ercanoglu, M., Gokceoglu, C., and Van Asch, Th. W. J.: Landslide susceptibility zoning north of Yenice (NW Turkey) by multivariate statistical techniques, *Natural Hazards*, 32, 1–23, 2004.

Fabbri, A. G., Chung, C. J. F., Cendrero, A., and Remondo, J.: Is Prediction of Future Landslides Possible with a GIS?, *Natural Hazards*, 30, 487–499, 2003.

Fernandez, C. I., Del Castillo, T. F., El Hamdouni, R., and Montero, J. C.: Verification of landslide 10 susceptibility mapping: A case study, *Earth Surface Process and Landforms*, 24, 537–544, 1999.

Gokceoglu, C. and Aksoy, H.: Landslide susceptibility mapping of the slopes in the residual soils of the Mengen region (Turkey) by deterministic stability analyses and image processing techniques, *Eng. Geol.*, 44, 147–161, 1996.

15 Gomez, H. and Kavzoglu, T.: Assessment of shallow landslide susceptibility using artificial neural networks in Jabonosa River Basin, Venezuela, *Engineering Geology*, doi:10.1016/j.enggeo.2004.10.004, in press, 2004.

Gritzner, M. L., Marcus, W. A., Aspinall, R., and Custer, S. G.: Assessing landslide potential 20 using GIS, soil wetness modeling and topographic attributes, Payette River, Idaho. *Geomorphology*, 37, 149–165, 2001.

Gupta, R. P. and Joshi, B. C.: Landslide hazard zoning using the GIS approach – A case study from the Ramganga Catchment, Himalayas, *Engineering Geology*, 28, 119–131, 1990.

Guzzetti, F., Carrara, A., Cardinali, M., and Reichenbach, P.: Landslide hazard evaluation: a 25 review of current techniques and their application in a multi-scale study, Central Italy, *Geomorphology*, 31, 181–216, 1999.

Guzzetti, F., Cardinali, M., Reichenbach, P., and Carrara, A.: Comparing landslide maps: A case study in the Upper Tiber River Basin, Central Italy, *Environmental Management*, 25, 3, 247–263, 2000.

<http://istanbul.meteor.gov.tr>: Website of State Meteorological Organisation, 2004.

30 Ildir, B.: Turkiyede heyelanların dagilimi ve afetler yasasi ile ilgili uygulamalar, In: Proc. Of 2nd National Landslide Symposium of Turkey, Sakarya University, 1–9, 1995 (in Turkish).

Jade, S. and Sarkar, S.: Statistical models for slope instability classification, *Engineering Geology*, 36, 91–98, 1993.

## Landslide susceptibility mapping of Cekmece

T. Y. Duman et al.

[Title Page](#)

[Abstract](#)

[Introduction](#)

[Conclusions](#)

[References](#)

[Tables](#)

[Figures](#)

[◀](#)

[▶](#)

[◀](#)

[▶](#)

[Back](#)

[Close](#)

[Full Screen / Esc](#)

[Print Version](#)

[Interactive Discussion](#)

EGU

Jager, S. and Wieczorek, G. F.: Landslide susceptibility in the Tully Valley Area, Finger Lakes Region, U.S. Geological Survey, Open-File Report 94-615, 1994.

Jakob, M.: The impacts of logging on landslide activity at Clayoquot Sound, British Columbia, *Catena* 38, 279–300, 2000.

5 Juang, C. H., Lee, D. H., and Sheu, C.: Mapping slope failure potential using fuzzy sets, *J. Geotech. Eng. Div., ASCE* 118, 475–493, 1992.

Koukis, G. and Ziourkas, C.: Slope instability phenomena in Greece: A statistical analysis, *Bulletin of International Association of Engineering Geologists*, 43, 47–60, 1991.

10 Lee, S.: Application of Likelihood Ratio and Logistic Regression Models to Landslide Susceptibility Mapping Using GIS, *Environmental Management*, 34, 223–232, 2004.

Lee, S. and Min, K.: Statistical analysis of landslide susceptibility at Yongin, Korea *Environ. Geol.*, 40, 1095–1113, 2001.

Lee, C. F., Ye, H., Yeung, M. R., Shan, X., and Chen, G.: AIGIS based methodology for natural terrain landslide susceptibility mapping in Hong Kong, *Episodes*, 24, 3, 150–159, 2001.

15 Lee, S., Ryu, J. H., Min, K., and Won, J. S.: Landslide susceptibility analysis using GIS and artificial neural network, *Earth Surf., Processes Landf.*, 28, 1361–1376, 2003.

Lee, S., Ryu, J. H., Won, J. S., and Park, H. J.: Determination and application of the weights for landslide susceptibility mapping using an artificial neural network, *Eng. Geol.*, 71, 289–302, 2004.

20 Luzzi, L. and Pergalani, F.: Slope instability in static and dynamic conditions for urban planning: the “Oltre Po Pavese” case history (Regione Lombardia-Italy), *Natural Hazards*, 20, 57–82, 1999.

Maharaj, R.: Landslide processes and landslide susceptibility analysis from an upland watershed: A case study from St. Andrew, Jamaica, West Indies, *Engineering Geology*, 34, 53–79, 1993.

25 Nagarajan, R., Roy, A., Vinod Kumar, R., Mukherjee, A., and Khire, M. V.: Landslide hazard susceptibility mapping based on terrain and climatic factors for tropical monsoon regions, *Bulletin of Engineering Geology and the Environment*, 58, 275–287, 2000.

Negnevitsky, M.: *Artificial Intelligence – A Guide to Intelligent Systems*, Addison – Wesley Co., Great Britain, 394, 2002.

30 Pachauri, A. K. and Pant, M.: Landslide hazard mapping based on geological attributes, *Engineering Geology*, 32, 81–100, 1992.

Pachauri, A. K., Gupta, P. V., and Chander, R.: Landslide zoning in a part of the Garhwal

## Landslide susceptibility mapping of Cekmece

T. Y. Duman et al.

[Title Page](#)

[Abstract](#)

[Introduction](#)

[Conclusions](#)

[References](#)

[Tables](#)

[Figures](#)

[◀](#)

[▶](#)

[◀](#)

[▶](#)

[Back](#)

[Close](#)

[Full Screen / Esc](#)

[Print Version](#)

[Interactive Discussion](#)

EGU

Himalayas, *Environmental Geology*, 36, 3–4, 325–334, 1998.

Parsons, T., Stein, R. S., Barka, A. A., Dieterich, J. H.: Heightened odds of large earthquakes near Istanbul; an interaction – based probability calculation, *Sci. Mag.*, April 28, 661–665, 2000.

5 Pistocchi, A., Luzi, L., and Napolitano, P.: The use of predictive modeling techniques for optimal exploitation of spatial databases: a case study in landslide hazard mapping with expert system – like methods, *Environmental Geology*, 41, 765–775, 2002.

Roth, R. A.: Factors affecting landslide susceptibility in San Mateo County, California, *Bulletin of the Association of Engineering Geologists*, XX, 4, 353–372, 1983.

10 Rowbotham, D. N. and Dudycha, D.: GIS modelling of slope stability in Phewa Tal watershed, Nepal, *Geomorphology*, 26, 151–170, 1998.

Safak, U., Avsar, N., and Meric, E.: Bati Bakirkoy (Istanbul) Tersiyer cokellerinin ostrakod ve formanifer toplulugu, *MTA Journal*, 121, 17–31, 1999 (in Turkish).

15 Soeters, R. S. and Van Westen, C. J.: Slope instability recognition, analysis and zonation, In: *Landslides: Investigation and Mitigation*, edited by Turner A. K. and Schuster, R. L., Transportation Research Board, Special Report, National Academy Press, Washington, C, 247, 129–177, 1996.

Soysal, H., Sipahioglu, S., Kolcak, D., and Altinok, Y.: *Tuurkiye ve Cevresinin Tarihsel Deprem Katalogu* (MO 2100–MS 1900), TUBITAK project Tbag 341, Istanbul, 1981.

20 Suzen, M. L. and Doyuran, V.: A comparison of the GIS based landslide susceptibility assessment methods: multivariate versus bivariate, *Environmental Geology*, 45, 665–679, 2004a.

Suzen, M. L. and Doyuran, V.: Data driven bivariate landslide susceptibility assessment using geographical information systems: a method and application to Asarsuyu catchment, Turkey, *Eng. Geol.*, 71, 303–321, 2004b.

25 Todd, D. C.: *Groundwater Hydrology*, John Wiley and Sons, New York, 336, 1980.

Turriini, M. C. and Visintainer, P.: Proposal of a method to define areas of landslide hazard and application to an area of the Dolomites, Italy, *Engineering Geology*, 50, 255–265, 1998.

Van Westen, C. J., Seijmonsbergen, A. C., and Mantovani, F.: Comparing landslide hazard maps, *Natural Hazards*, 20, 137–158, 1999.

30 Varnes, D. J.: Slope movement types and processes, In: *Landslides Analysis and Control*, edited by Schuster, R. L. and Krizek, R. J., Special Report, Transportation Research Board, National Academy of Sciences, New York, 176, 12–33, 1978.

Wachal, D. J. and Hudak, P. F.: Mapping landslide susceptibility in Travis County, Texas, USA,

Geo. Journal, 51, 245–253, 2000.

WP/WLI (Working Party on World Landslide Inventory): A suggested method for describing the activity of a landslide, Bull. Int. Assoc. Eng. Geol., 47, 53–57, 1993.

Zeze, J. L.: Landslide susceptibility assessment considering landslide typology. A case study in the area north of Lisbon (Portugal), Natural Hazards and Earth System Sciences, 2, 73–82, 2002, [SRef-ID: 1684-9981/nhess/2002-2-73](#).

Zeze, J. L., Ferreira, A. B., and Rodrigues, M. L.: Landslides in the North of Lisbon Region (Portugal): Conditioning and triggering factors, Physical and Chemical Earth (A), 24, 10, 925–934, 1999.

5

10

HESSD

2, 155–208, 2005

---

Landslide  
susceptibility  
mapping of Cekmece

T. Y. Duman et al.

---

[Title Page](#)

[Abstract](#)

[Introduction](#)

[Conclusions](#)

[References](#)

[Tables](#)

[Figures](#)

◀

▶

◀

▶

[Back](#)

[Close](#)

[Full Screen / Esc](#)

[Print Version](#)

[Interactive Discussion](#)

EGU

**Table 1.** The data employed in the analyses and the results obtained from the conditional probability approach.

Parameter	Parameter class area			Landslide area in parameter class					
	Pix.	Count.	$m^2$	Pix.	Count.	$m^2$	$P(A B_i)$	$P(B_i)$	$P(A)$
<b>Slope (°)</b>									
0–5	152235	95146875	13078	8173750	0.085907	0.543440	0.046685		
5–10	96444	60277500	26665	16665625	0.276482	0.344281	0.095187		
10–15	22221	13888125	9389	5868125	0.422528	0.079323	0.033516		
15–20	5959	3724375	2851	1781875	0.478436	0.021272	0.010177		
20–25	1980	1237500	1011	631875	0.510606	0.007068	0.003609		
25–30	767	479375	402	251250	0.524120	0.002738	0.001435		
30–50	520	325000	275	171875	0.528846	0.001856	0.000982		
50–90	6	3750	3	1875	0.500000	0.000021	0.000011		
<b>Aspect (°)</b>									
0–45	18323	11451875	4075	2546875	0.222398	0.065408	0.014547		
45–90	38150	23843750	6521	4075625	0.170931	0.136186	0.023278		
90–135	33985	21240625	5203	3251875	0.153097	0.121318	0.018573		
135–180	29140	18212500	6671	4169375	0.228929	0.104022	0.023814		
180–225	29119	18199375	7733	4833125	0.265565	0.103947	0.027605		
225–270	41964	26227500	7706	4816250	0.183634	0.149801	0.027508		
270–315	33657	21035625	6920	4325000	0.205604	0.120147	0.024703		
315–360	17597	10998125	3693	2308125	0.209865	0.062817	0.013183		
-1	38197	23873125	5152	3220000	0.134880	0.136354	0.018391		

## Landslide susceptibility mapping of Çekmecé

T. Y. Duman et al.

[Title Page](#)

[Abstract](#)

[Introduction](#)

[Conclusions](#)

[References](#)

[Tables](#)

[Figures](#)

[◀](#)

[▶](#)

[◀](#)

[▶](#)

[Back](#)

[Close](#)

[Full Screen / Esc](#)

[Print Version](#)

[Interactive Discussion](#)

EGU

**Table 1.** Continued.

Parameter	Parameter class area			Landslide area in parameter class			
	Pix. Count.	$m^2$	Pix. Count.	$m^2$	$P(A/B_i)$	$P(B_i)$	$P(A)$
<b>Altitude (m)</b>							
0–25	28974	18108750	4862	3038750	0.167806	0.103430	0.017356
25–50	37867	23666875	9930	6206250	0.262234	0.135176	0.035448
50–75	37542	23463750	9526	5953750	0.253742	0.134015	0.034005
75–100	43156	26972500	8829	5518125	0.204583	0.154056	0.031517
100–125	43277	27048125	8164	5102500	0.188645	0.154488	0.029143
125–150	39680	24800000	7352	4595000	0.185282	0.141648	0.026245
150–175	32089	20055625	4467	2791875	0.139207	0.114550	0.015946
175–200	17547	10966875	544	340000	0.031002	0.062638	0.001942
<b>Lithology</b>							
Qa	15644	9777500	1127	704375	0.072040	0.055845	0.004023
Tek	1613	1008125	0	0	0.000000	0.005758	0.000000
Teoi	43337	27085625	1810	1131250	0.041766	0.154702	0.006461
Teoi2	478	298750	66	41250	0.138075	0.001706	0.000236
Teoiy	1035	646875	0	0	0.000000	0.003695	0.000000
Tmb	56253	35158125	4473	2795625	0.079516	0.200809	0.015967
Tme	71366	44603750	13617	8510625	0.190805	0.254758	0.048609
To	14336	8960000	5706	3566250	0.398019	0.051176	0.020369
Tod	20650	12906250	4728	2955000	0.228959	0.073715	0.016878
Toda	34254	21408750	17151	10719375	0.500701	0.122278	0.061225
Tos	21166	13228750	4996	3122500	0.236039	0.075557	0.017834

## Landslide susceptibility mapping of Cekmece

T. Y. Duman et al.

Title Page

Abstract

Introduction

Conclusions

References

Tables

Figures

◀

▶

◀

▶

Back

Close

Full Screen / Esc

Print Version

Interactive Discussion

EGU

**Table 1.** Continued.

Parameter	Parameter class area			Landslide area in parameter class		
	Pix.	Count.	$m^2$	Pix.	Count.	$m^2$
	P(A/ $B_i$ )	P( $B_i$ )	P(A)			
<b>Geomorphology</b>						
AB	385	240625	0	0	0.000000	0.001374
By	128	80000	69	43125	0.539063	0.000457
Db	231	144375	76	47500	0.329004	0.000825
Dko	1754	1096250	57	35625	0.032497	0.006261
Dp	207	129375	0	0	0.000000	0.000739
EKSY	1004	627500	0	0	0.000000	0.003584
EL	1296	810000	6	3750	0.004630	0.004626
HB	1387	866875	144	90000	0.103821	0.004951
PH	3511	2194375	1071	669375	0.305041	0.012533
UMAY	1356	847500	1	625	0.000737	0.004841
UMDY	67225	42015625	1566	978750	0.023295	0.239976
Vt	9845	6153125	420	262500	0.042661	0.035144
Y	184517	115323125	50242	31401250	0.272289	0.658679
YK	91	56875	21	13125	0.230769	0.000325
<b>Dist. Fr. Faults (m)</b>						
0–200	22328	13955000	1009	630625	0.045190	0.079705
200–400	19180	11987500	1150	718750	0.059958	0.068468
400–600	14661	9163125	1251	781875	0.085328	0.052336
600–800	13224	8265000	1567	979375	0.118497	0.047206
800–1000	11443	7151875	1604	1002500	0.140173	0.040849
						0.005726

## Landslide susceptibility mapping of Cekmec

T. Y. Duman et al.

[Title Page](#)[Abstract](#)[Introduction](#)[Conclusions](#)[References](#)[Tables](#)[Figures](#)[◀](#)[▶](#)[◀](#)[▶](#)[Back](#)[Close](#)[Full Screen / Esc](#)[Print Version](#)[Interactive Discussion](#)

EGU

**Table 1.** Continued.

Parameter	Parameter class area			Landslide area in parameter class			
	Pix. Count.	$m^2$	Pix. Count.	$m^2$	$P(A/B_i)$	$P(B_i)$	$P(A)$
<b>Dist. Fr. Drain. (m)</b>							
0–25	6855	4284375	1066	666250	0.155507	0.024471	0.003805
25–50	6810	4256250	1571	981875	0.230690	0.024310	0.005608
50–75	6714	4196250	1763	1101875	0.262586	0.023967	0.006293
75–100	6590	4118750	1792	1120000	0.271927	0.023525	0.006397
100–125	6578	4111250	1691	1056875	0.257069	0.023482	0.006036
<b>Dist. Fr. Roads (m)</b>							
0–10	11531	7206875	1308	817500	0.113433	0.041163	0.004669
10–20	11197	6998125	1217	760625	0.108690	0.039970	0.004344
20–30	10141	6338125	1219	761875	0.120205	0.036201	0.004352
30–40	9972	6232500	1192	745000	0.119535	0.035598	0.004255
40–50	8976	5610000	1171	731875	0.130459	0.032042	0.004180
<b>Relative permeability</b>							
Low (or impermeable)	113571	70981875	29729	18580625	0.261766	0.405420	0.106125
Moderate	20650	12906250	4728	2955000	0.228959	0.073715	0.016878
High	145911	91194375	19217	12010625	0.131704	0.520865	0.068600

## Landslide susceptibility mapping of Cekmec

T. Y. Duman et al.

[Title Page](#)

[Abstract](#)

[Introduction](#)

[Conclusions](#)

[References](#)

[Tables](#)

[Figures](#)

◀

▶

[Back](#)

[Close](#)

[Full Screen / Esc](#)

[Print Version](#)

[Interactive Discussion](#)

EGU

## Landslide susceptibility mapping of Cekmece

T. Y. Duman et al.

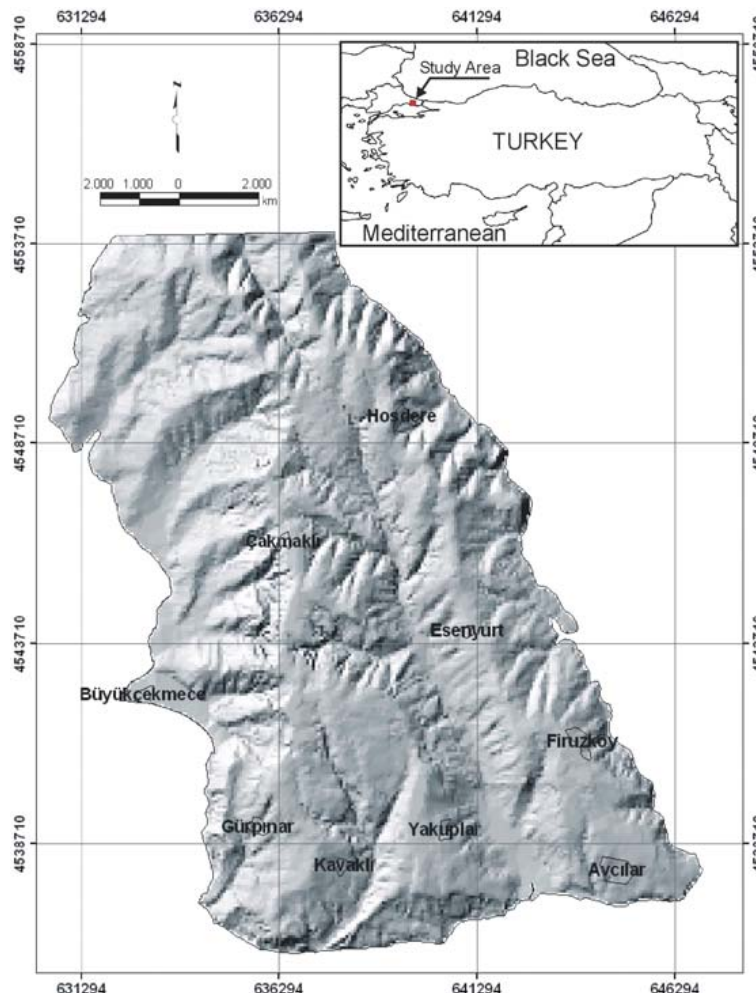


**Fig. 1.** Location map of the study area.

[Title Page](#)

[Abstract](#)

[Introduction](#)

[Conclusions](#)

[References](#)

[Tables](#)

[Figures](#)

[|◀](#)

[▶|](#)

[◀](#)

[▶](#)

[Back](#)

[Close](#)

[Full Screen / Esc](#)

[Print Version](#)

[Interactive Discussion](#)

## Landslide susceptibility mapping of Çekmece

T. Y. Duman et al.

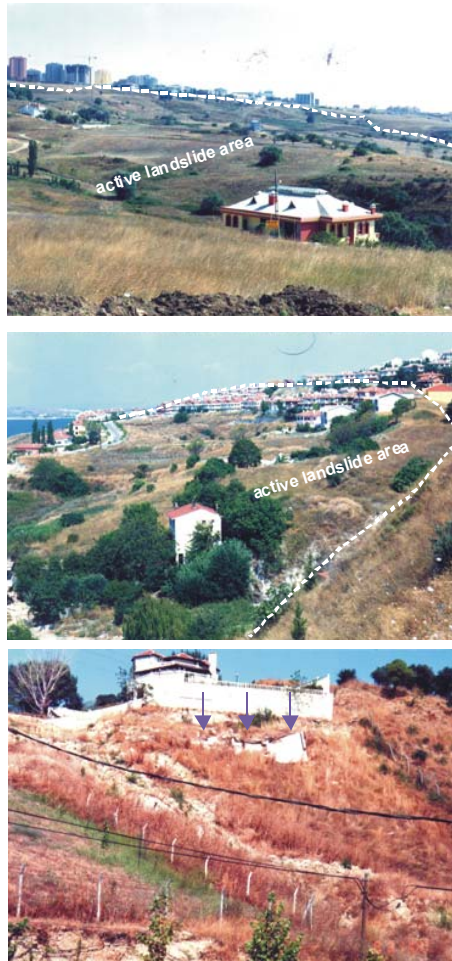


**Fig. 2.** Some typical views from the study area (many buildings were constructed in the active landslides).

[Title Page](#)

[Abstract](#)

[Introduction](#)

[Conclusions](#)

[References](#)

[Tables](#)

[Figures](#)

◀

▶

◀

▶

[Back](#)

[Close](#)

[Full Screen / Esc](#)

[Print Version](#)

[Interactive Discussion](#)

## Landslide susceptibility mapping of Cekmece

T. Y. Duman et al.

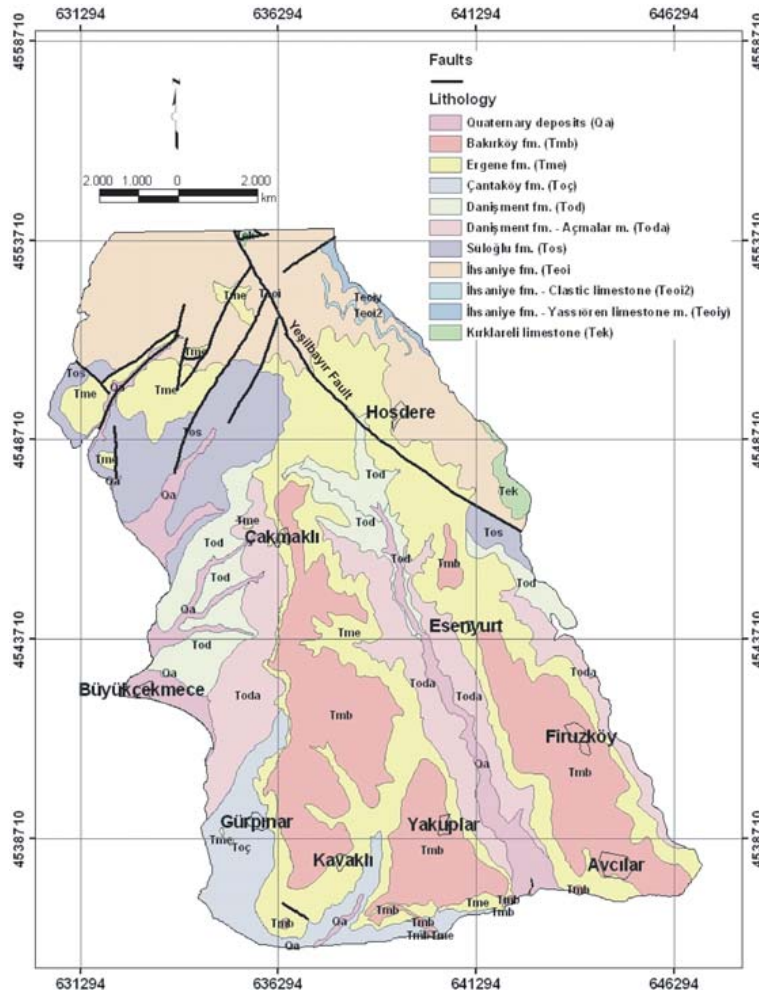


Fig. 3. Geological map of the study area (Duman et al., 2004a).

[Title Page](#)

[Abstract](#)

[Introduction](#)

[Conclusions](#)

[References](#)

[Tables](#)

[Figures](#)

[◀](#)

[▶](#)

[◀](#)

[▶](#)

[Back](#)

[Close](#)

[Full Screen / Esc](#)

[Print Version](#)

[Interactive Discussion](#)

## Landslide susceptibility mapping of Cekmece

T. Y. Duman et al.



**Fig. 4.** A close view from the Danismert formation.

[Title Page](#)

[Abstract](#)

[Introduction](#)

[Conclusions](#)

[References](#)

[Tables](#)

[Figures](#)

◀

▶

◀

▶

[Back](#)

[Close](#)

[Full Screen / Esc](#)

[Print Version](#)

[Interactive Discussion](#)

EGU

## Landslide susceptibility mapping of Cekmece

T. Y. Duman et al.

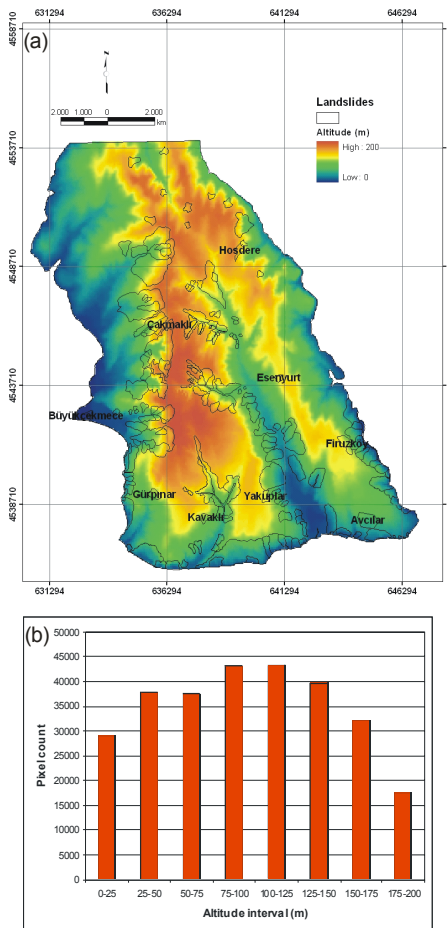


**Fig. 5.** (a) Altitude map of the study area and (b) Histogram showing the distribution of altitude values of the study area.

[Title Page](#)

[Abstract](#)

[Introduction](#)

[Conclusions](#)

[References](#)

[Tables](#)

[Figures](#)

[◀](#)

[▶](#)

[◀](#)

[▶](#)

[Back](#)

[Close](#)

[Full Screen / Esc](#)

[Print Version](#)

[Interactive Discussion](#)

## Landslide susceptibility mapping of Cekmece

T. Y. Duman et al.

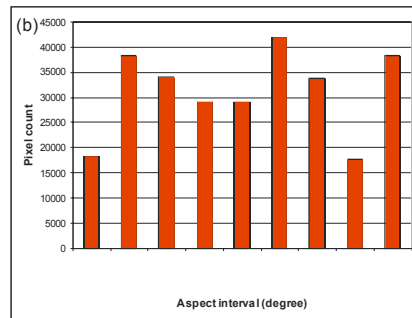
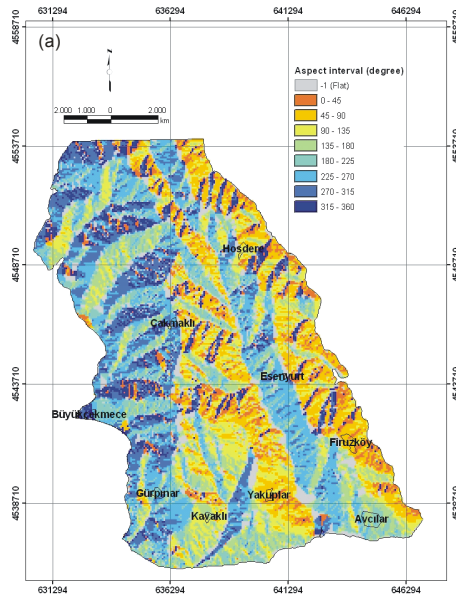


**Fig. 6.** (a) Aspect map of the study area and (b) Histogram showing the distribution of the aspect values of the study area.

[Title Page](#)

[Abstract](#)

[Introduction](#)

[Conclusions](#)

[References](#)

[Tables](#)

[Figures](#)

◀

▶

◀

▶

[Back](#)

[Close](#)

[Full Screen / Esc](#)

[Print Version](#)

[Interactive Discussion](#)

## Landslide susceptibility mapping of Cekmece

T. Y. Duman et al.

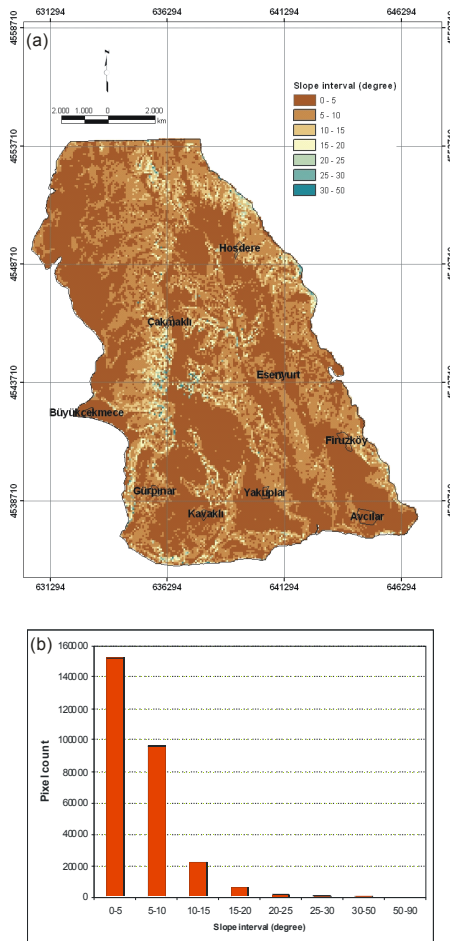


**Fig. 7.** (a) Slope map of the study area and (b) Histogram showing the distribution of the slope values of the study area.

[Title Page](#)

[Abstract](#)

[Introduction](#)

[Conclusions](#)

[References](#)

[Tables](#)

[Figures](#)

◀

▶

◀

▶

[Back](#)

[Close](#)

[Full Screen / Esc](#)

[Print Version](#)

[Interactive Discussion](#)

## Landslide susceptibility mapping of Cekmece

T. Y. Duman et al.

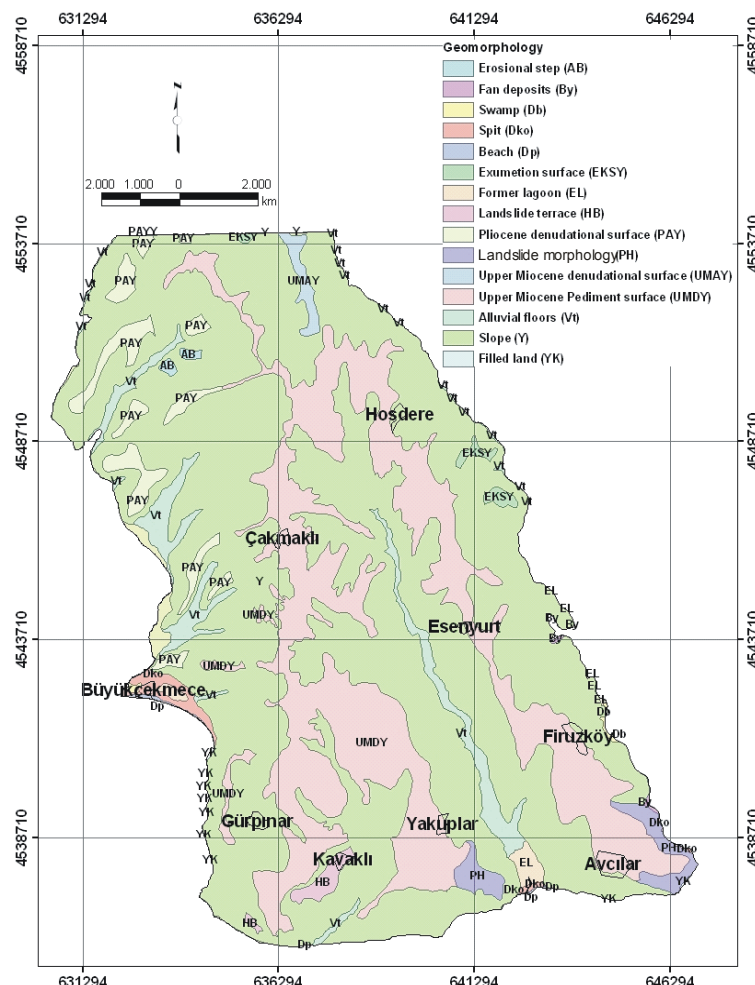
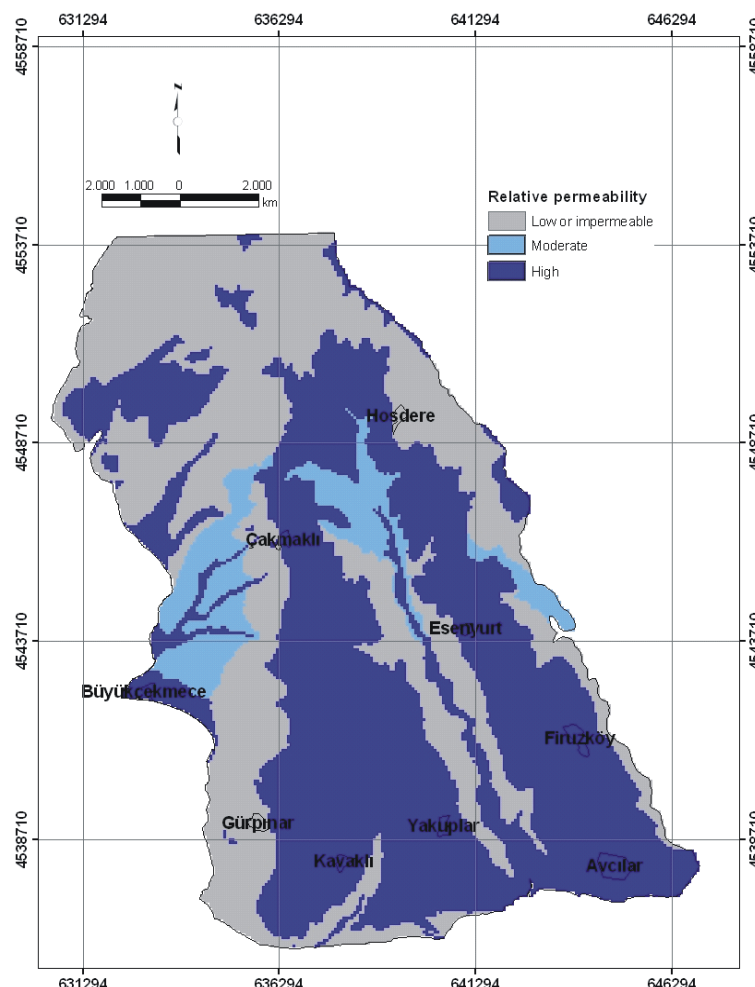


Fig. 8. Geomorphology map of the study area (Duman et al., 2004a).

- [Title Page](#)
- [Abstract](#) [Introduction](#)
- [Conclusions](#) [References](#)
- [Tables](#) [Figures](#)
- [◀](#) [▶](#)
- [◀](#) [▶](#)
- [Back](#) [Close](#)
- [Full Screen / Esc](#)
- [Print Version](#)
- [Interactive Discussion](#)

**Landslide  
susceptibility  
mapping of Cekmece**

T. Y. Duman et al.



**Fig. 9.** Relative permeability map of the lithologies (Duman et al., 2004a).

- [Title Page](#)
- [Abstract](#) [Introduction](#)
- [Conclusions](#) [References](#)
- [Tables](#) [Figures](#)
- [◀](#) [▶](#)
- [◀](#) [▶](#)
- [Back](#) [Close](#)
- [Full Screen / Esc](#)
- [Print Version](#)
- [Interactive Discussion](#)

## Landslide susceptibility mapping of Cekmec

T. Y. Duman et al.

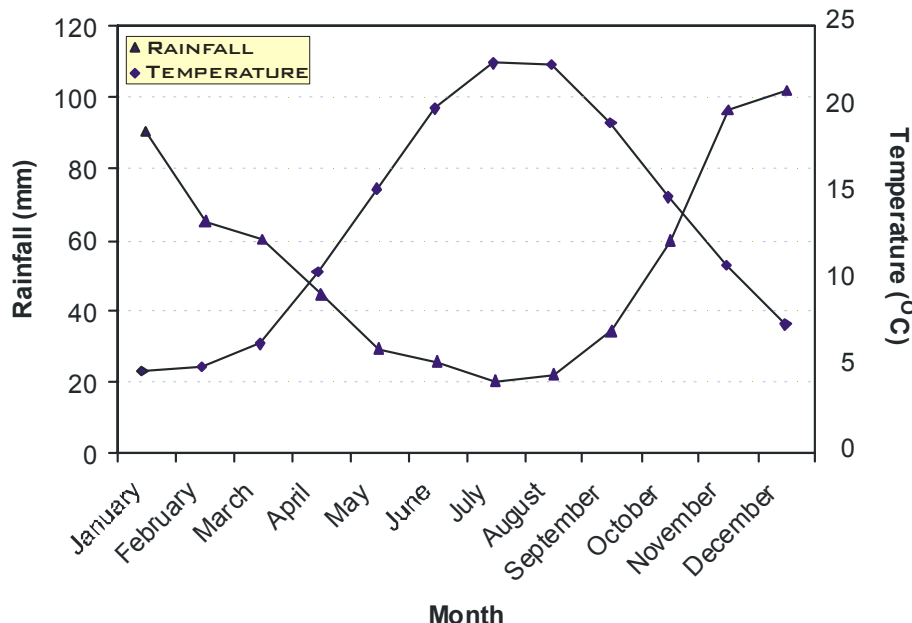


**Fig. 10.** Average annual rainfall and temperature graph of the data from Florya Meteorology Station.

- [Title Page](#)
- [Abstract](#) [Introduction](#)
- [Conclusions](#) [References](#)
- [Tables](#) [Figures](#)
- [◀](#) [▶](#)
- [◀](#) [▶](#)
- [Back](#) [Close](#)
- [Full Screen / Esc](#)
- [Print Version](#)
- [Interactive Discussion](#)

**Landslide  
susceptibility  
mapping of Cekmecé**

T. Y. Duman et al.

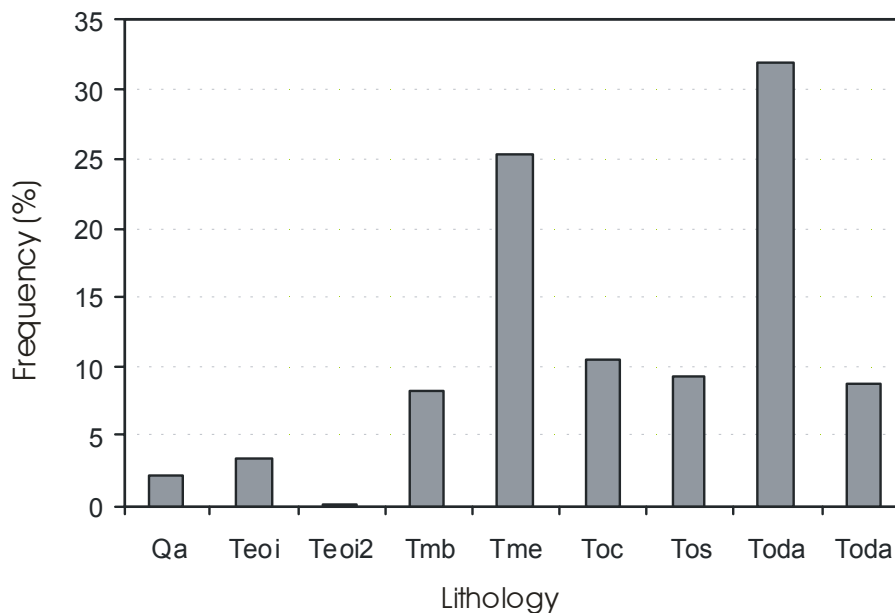


**Fig. 11.** Histogram illustrating the distribution of the landslides with respect to the lithologies at the study area.

- [Title Page](#)
- [Abstract](#) [Introduction](#)
- [Conclusions](#) [References](#)
- [Tables](#) [Figures](#)
- [◀](#) [▶](#)
- [◀](#) [▶](#)
- [Back](#) [Close](#)
- [Full Screen / Esc](#)
- [Print Version](#)
- [Interactive Discussion](#)

## Landslide susceptibility mapping of Cekmece

T. Y. Duman et al.



**Fig. 12.** A large landslide identified in the area.

[Title Page](#)

[Abstract](#)

[Introduction](#)

[Conclusions](#)

[References](#)

[Tables](#)

[Figures](#)

◀

▶

◀

▶

[Back](#)

[Close](#)

[Full Screen / Esc](#)

[Print Version](#)

[Interactive Discussion](#)

EGU

**Landslide  
susceptibility  
mapping of Cekmece**

T. Y. Duman et al.

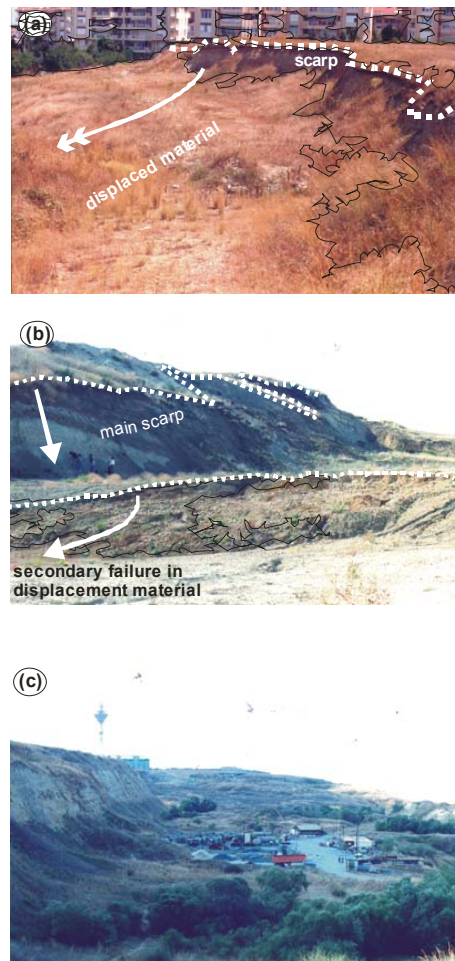


**Fig. 13.** Some typical views from the landslides in the area.

[Title Page](#)[Abstract](#)[Introduction](#)[Conclusions](#)[References](#)[Tables](#)[Figures](#)[|◀](#)[▶|](#)[◀](#)[▶](#)[Back](#)[Close](#)[Full Screen / Esc](#)[Print Version](#)[Interactive Discussion](#)

**Landslide  
susceptibility  
mapping of Cekmece**

T. Y. Duman et al.

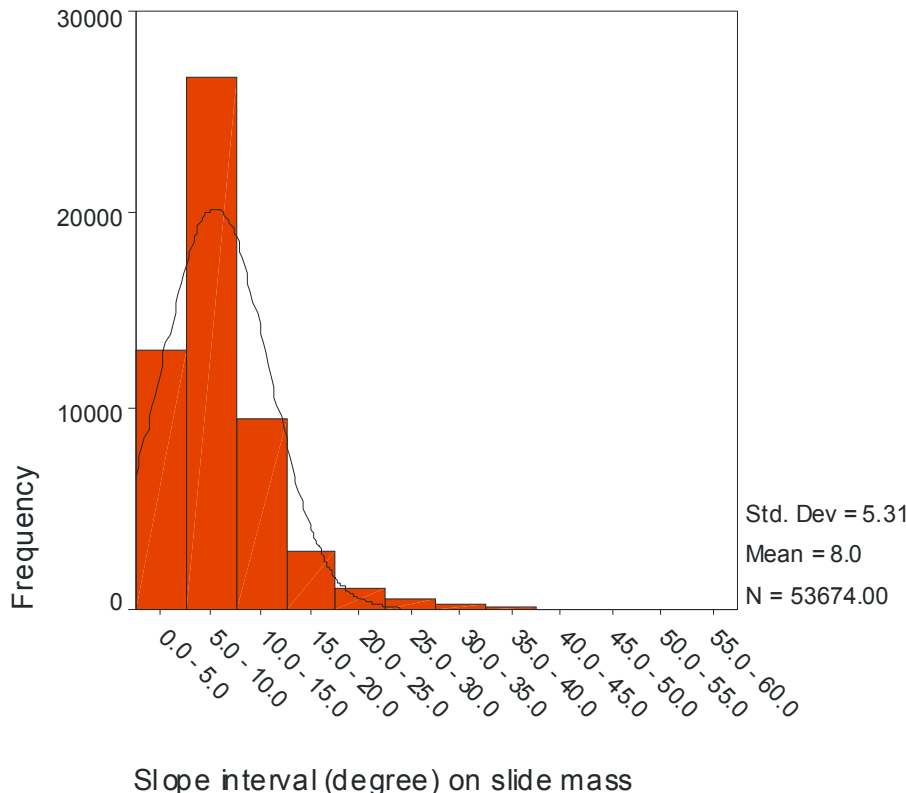


**Fig. 14.** Histogram illustrating the distribution of the landslides with respect to the slope angle at the study area.

- [Title Page](#)
- [Abstract](#) [Introduction](#)
- [Conclusions](#) [References](#)
- [Tables](#) [Figures](#)
- [◀](#) [▶](#)
- [◀](#) [▶](#)
- [Back](#) [Close](#)
- [Full Screen / Esc](#)
- [Print Version](#)
- [Interactive Discussion](#)

**Landslide  
susceptibility  
mapping of Cekmece**

T. Y. Duman et al.

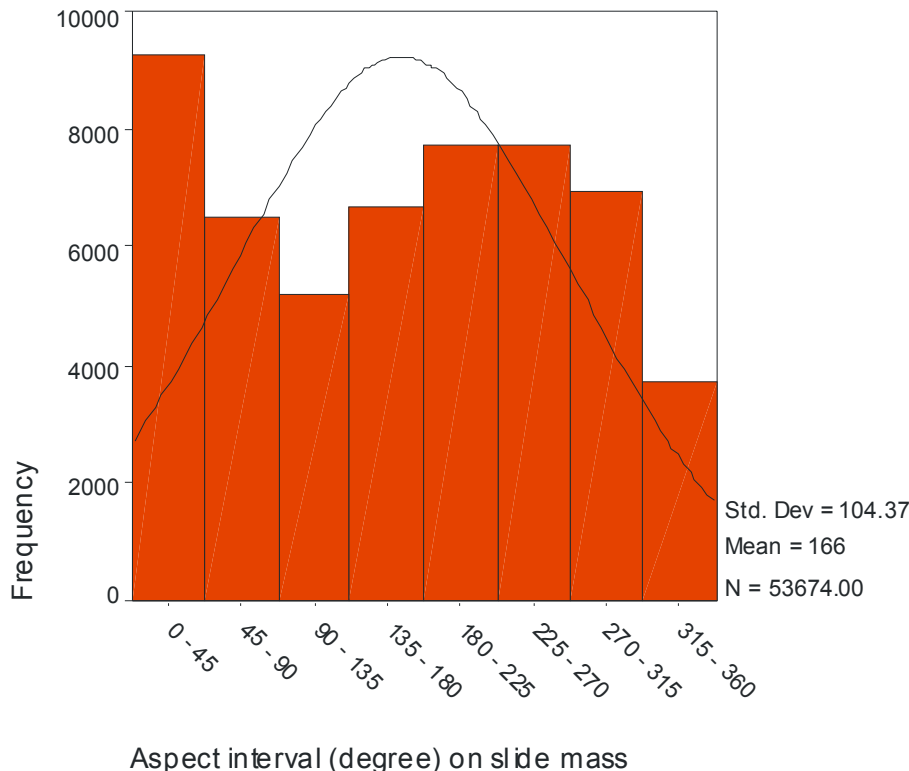


**Fig. 15.** Histogram illustrating the distribution of the landslides with respect to the aspect at the study area.

- [Title Page](#)
- [Abstract](#) [Introduction](#)
- [Conclusions](#) [References](#)
- [Tables](#) [Figures](#)
- [◀](#) [▶](#)
- [◀](#) [▶](#)
- [Back](#) [Close](#)
- [Full Screen / Esc](#)
- [Print Version](#)
- [Interactive Discussion](#)

## Landslide susceptibility mapping of Cekmec

T. Y. Duman et al.

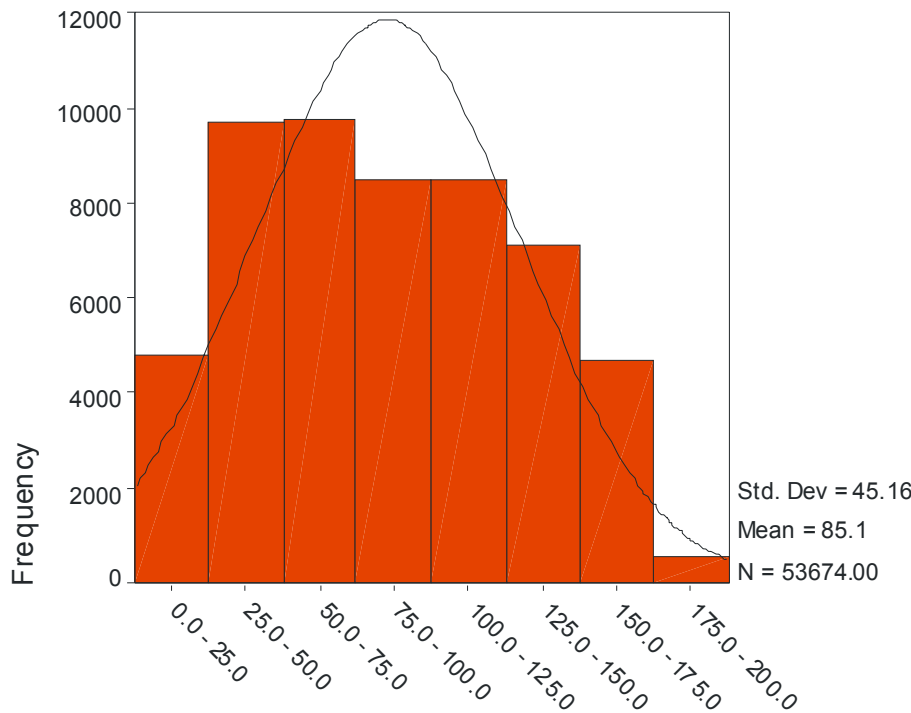


**Fig. 16.** Histogram illustrating the distribution of the landslides with respect to the altitude values at the study area.

- [Title Page](#)
- [Abstract](#) [Introduction](#)
- [Conclusions](#) [References](#)
- [Tables](#) [Figures](#)
- [◀](#) [▶](#)
- [◀](#) [▶](#)
- [Back](#) [Close](#)
- [Full Screen / Esc](#)
- [Print Version](#)
- [Interactive Discussion](#)

## Landslide susceptibility mapping of Çekmece

T. Y. Duman et al.

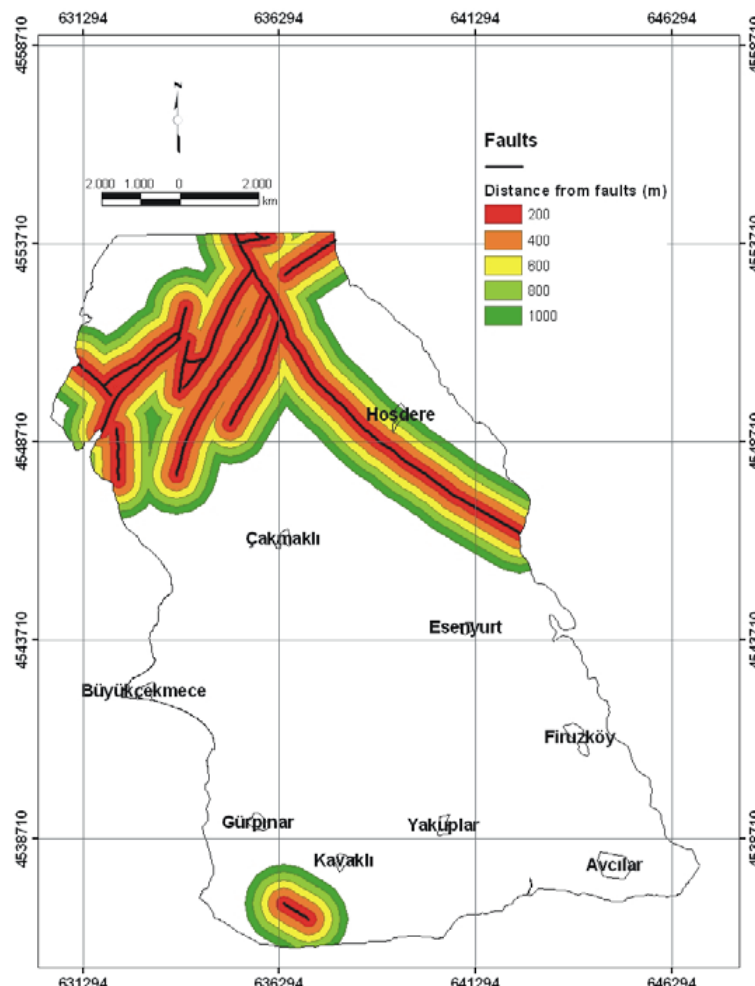


**Fig. 17.** The main faults and the buffer zones indicating to closeness to the faults.

- [Title Page](#)
- [Abstract](#) [Introduction](#)
- [Conclusions](#) [References](#)
- [Tables](#) [Figures](#)
- [◀](#) [▶](#)
- [◀](#) [▶](#)
- [Back](#) [Close](#)
- [Full Screen / Esc](#)
- [Print Version](#)
- [Interactive Discussion](#)

## Landslide susceptibility mapping of Cekmec

T. Y. Duman et al.

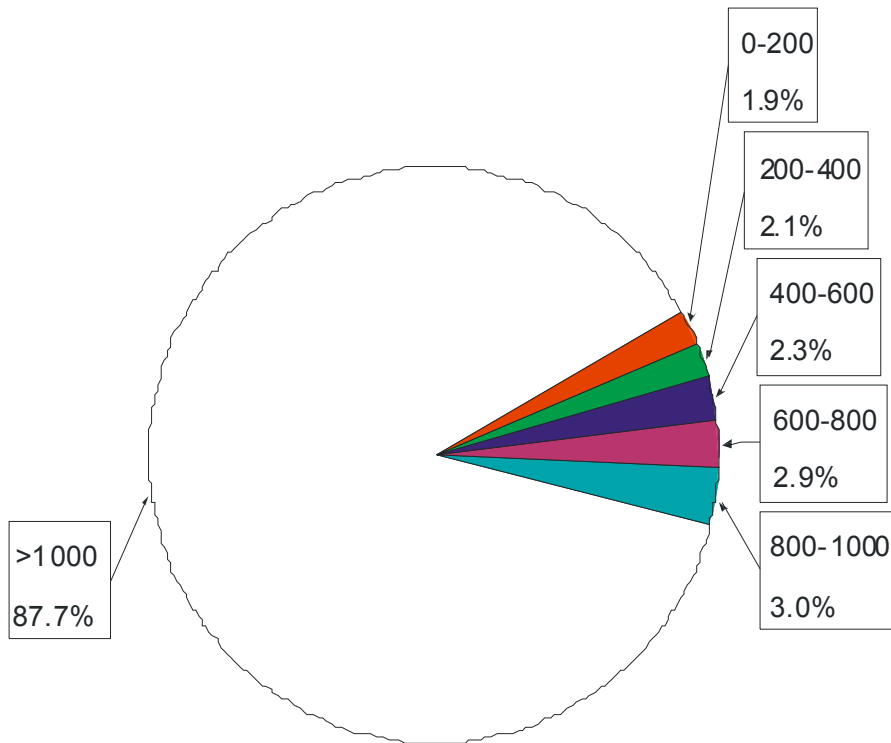


**Fig. 18.** Pie chart illustrating the distribution of the landslides with respect to the buffer zones indicating the closeness to the faults at the study area.

<a href="#">Title Page</a>	
<a href="#">Abstract</a>	<a href="#">Introduction</a>
<a href="#">Conclusions</a>	<a href="#">References</a>
<a href="#">Tables</a>	<a href="#">Figures</a>
<a href="#">◀</a>	<a href="#">▶</a>
<a href="#">◀</a>	<a href="#">▶</a>
<a href="#">Back</a>	<a href="#">Close</a>
<a href="#">Full Screen / Esc</a>	
<a href="#">Print Version</a>	
<a href="#">Interactive Discussion</a>	

## Landslide susceptibility mapping of Cekmece

T. Y. Duman et al.

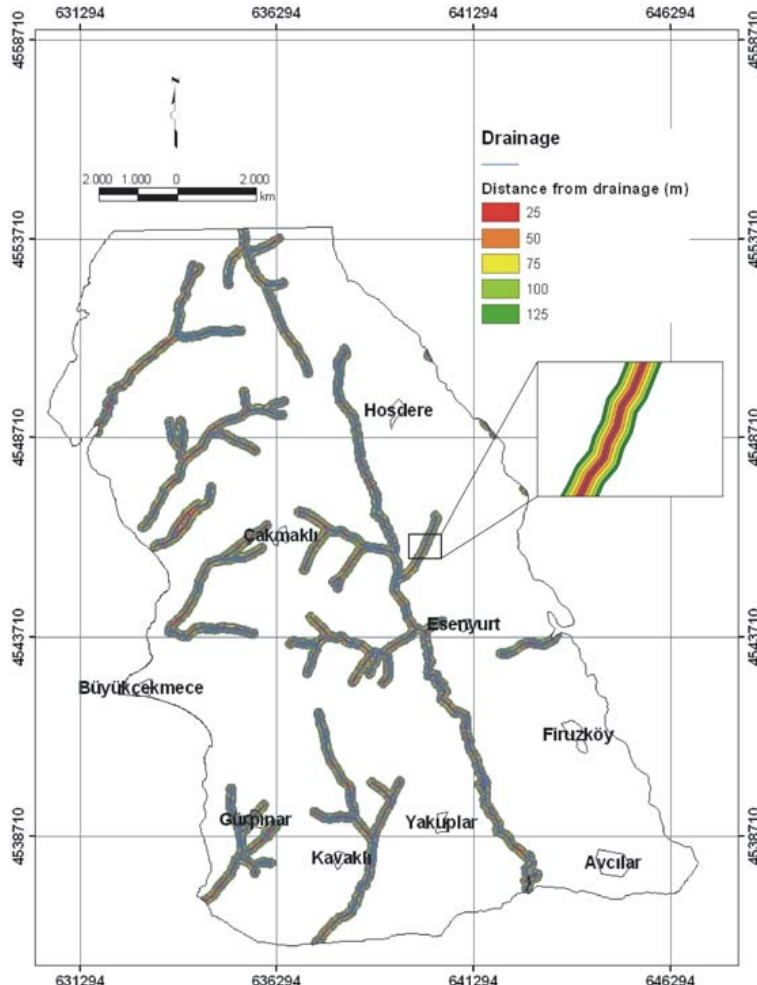


**Fig. 19.** The main drainage pattern and the buffer zones indicating the closeness to the drainage pattern.

- [Title Page](#)
- [Abstract](#) [Introduction](#)
- [Conclusions](#) [References](#)
- [Tables](#) [Figures](#)
- [◀](#) [▶](#)
- [◀](#) [▶](#)
- [Back](#) [Close](#)
- [Full Screen / Esc](#)
- [Print Version](#)
- [Interactive Discussion](#)

## Landslide susceptibility mapping of Cekmec

T. Y. Duman et al.

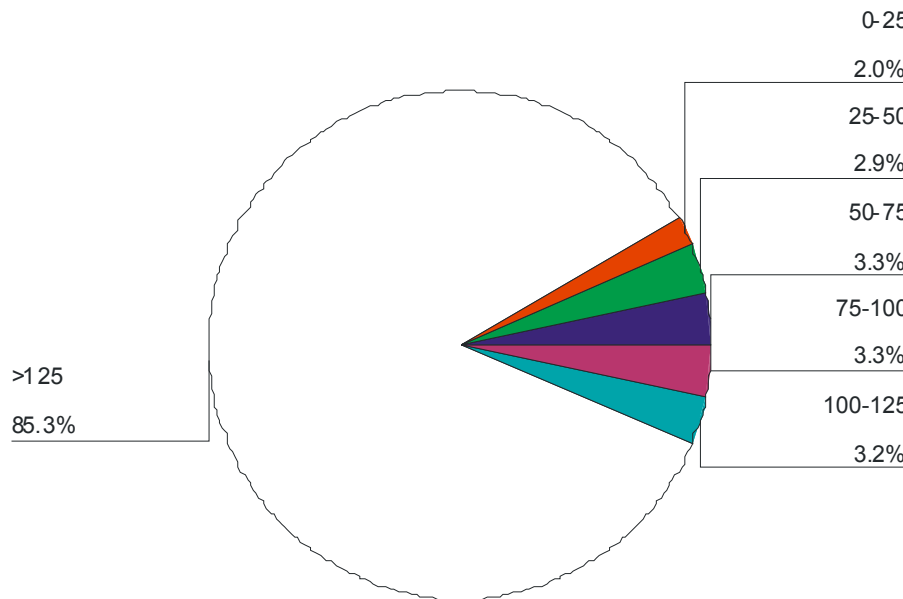


**Fig. 20.** Pie chart illustrating the distribution of the landslides with respect to the buffer zones indicating the closeness to the network at the study area.

Print Version

Interactive Discussion

EGU

## Landslide susceptibility mapping of Çekmece

T. Y. Duman et al.

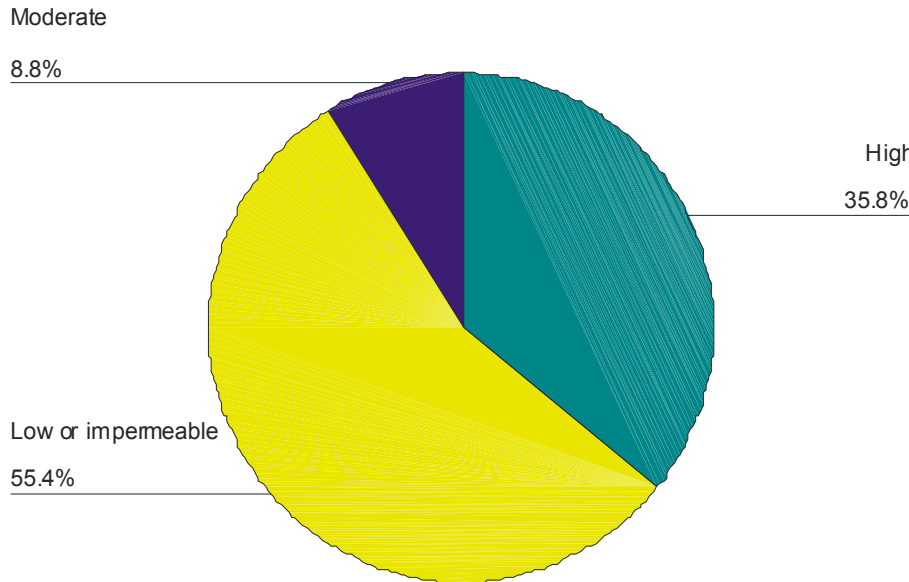


**Fig. 21.** Pie chart illustrating the distribution of the landslides with respect to the relative permeability classes of the lithologies network at the study area.

- [Title Page](#)
- [Abstract](#) [Introduction](#)
- [Conclusions](#) [References](#)
- [Tables](#) [Figures](#)
- [◀](#) [▶](#)
- [◀](#) [▶](#)
- [Back](#) [Close](#)
- [Full Screen / Esc](#)
- [Print Version](#)
- [Interactive Discussion](#)

## Landslide susceptibility mapping of Çekmece

T. Y. Duman et al.

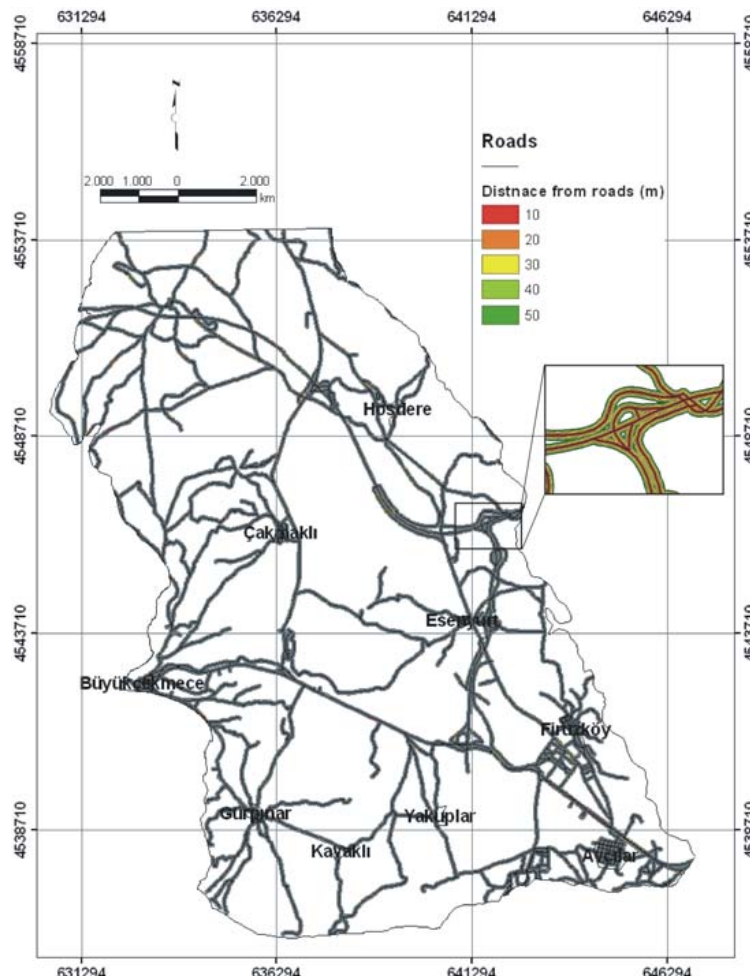


**Fig. 22.** The main road network and the buffer zones indicating the closeness to the main roads.

- [Title Page](#)
- [Abstract](#) [Introduction](#)
- [Conclusions](#) [References](#)
- [Tables](#) [Figures](#)
- [◀](#) [▶](#)
- [◀](#) [▶](#)
- [Back](#) [Close](#)
- [Full Screen / Esc](#)
- [Print Version](#)
- [Interactive Discussion](#)

**Landslide  
susceptibility  
mapping of Cekmecé**

T. Y. Duman et al.

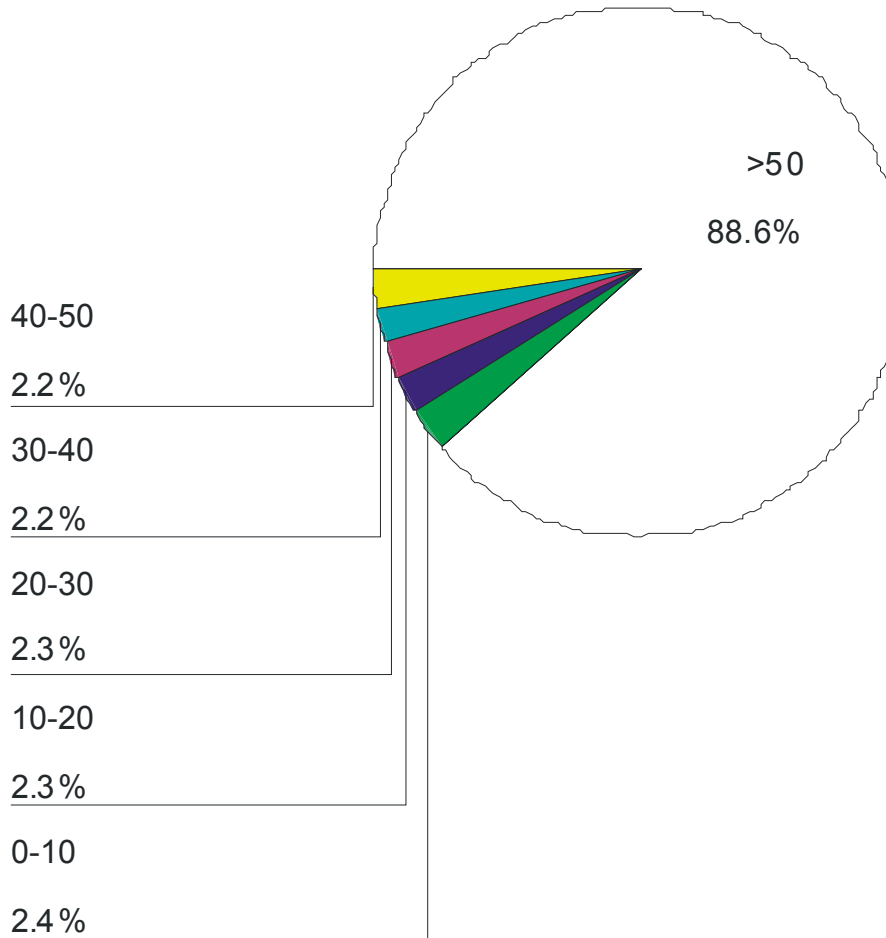


**Fig. 23.** Pie chart illustrating the distribution of the landslides with respect to the buffer zones indicating the closeness to the roads at the study area.

---

Landslide  
susceptibility  
mapping of Cekmece

T. Y. Duman et al.

---

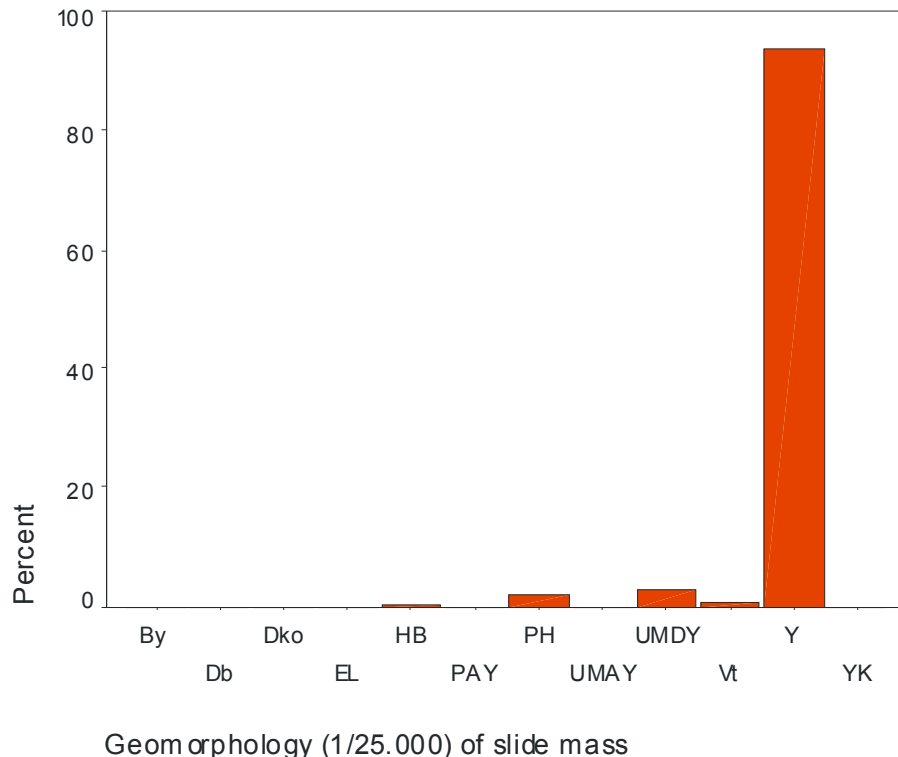


**Fig. 24.** Histogram illustrating the distribution of the landslides with respect to the geomorphological units at the study area.

- [Title Page](#)
- [Abstract](#) [Introduction](#)
- [Conclusions](#) [References](#)
- [Tables](#) [Figures](#)
- [◀](#) [▶](#)
- [◀](#) [▶](#)
- [Back](#) [Close](#)
- [Full Screen / Esc](#)
- [Print Version](#)
- [Interactive Discussion](#)

## Landslide susceptibility mapping of Cekmece

T. Y. Duman et al.

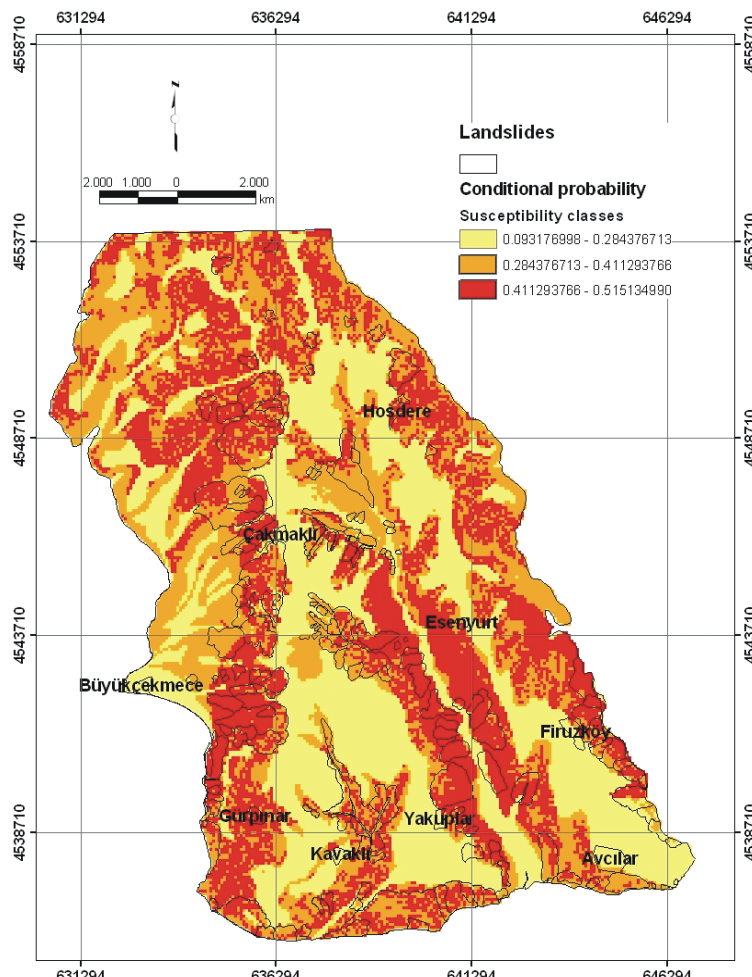
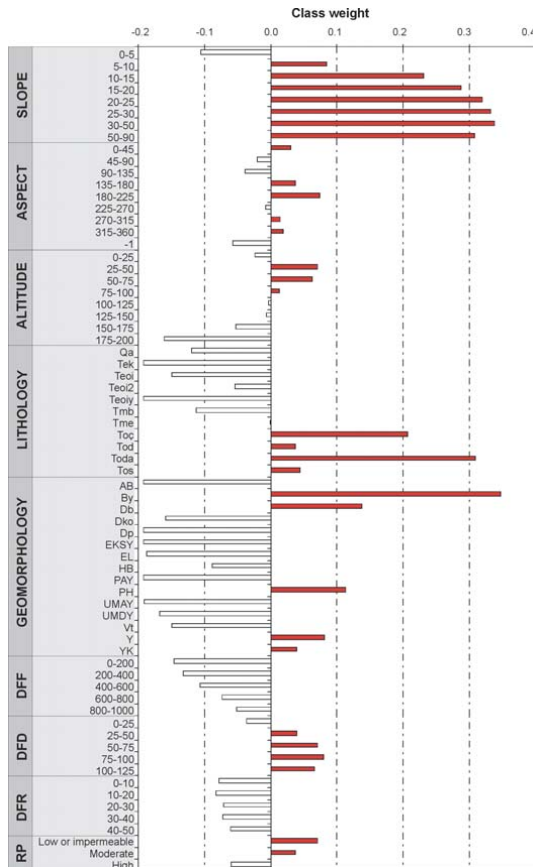


**Fig. 25.** Final landslide susceptibility map of the Cekmece (Istanbul) area.

- [Title Page](#)
- [Abstract](#) [Introduction](#)
- [Conclusions](#) [References](#)
- [Tables](#) [Figures](#)
- [◀](#) [▶](#)
- [◀](#) [▶](#)
- [Back](#) [Close](#)
- [Full Screen / Esc](#)
- [Print Version](#)
- [Interactive Discussion](#)

## Landslide susceptibility mapping of Cekmece

T. Y. Duman et al.

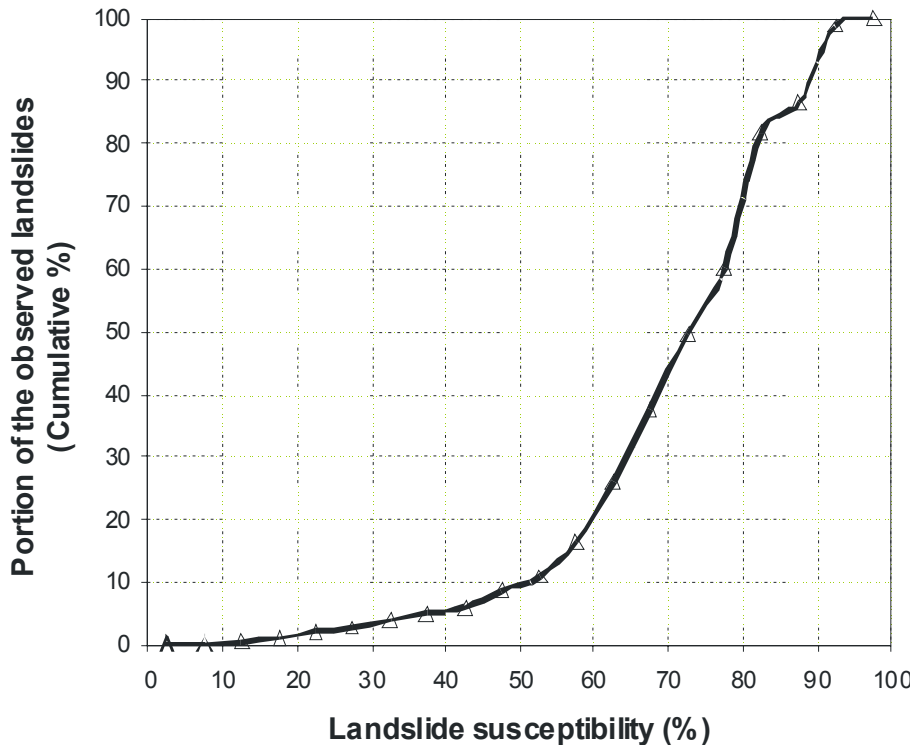


**Fig. 26.** Histogram showing the distribution of the weight values of the parameter classes.

EGU

**Landslide susceptibility mapping of Cekmece**

T. Y. Duman et al.

**Fig. 27.** Relation between the landslide susceptibility and portion of the observed landslides.

- [Title Page](#)
- [Abstract](#) [Introduction](#)
- [Conclusions](#) [References](#)
- [Tables](#) [Figures](#)
- [◀](#) [▶](#)
- [◀](#) [▶](#)
- [Back](#) [Close](#)
- [Full Screen / Esc](#)
- [Print Version](#)
- [Interactive Discussion](#)